Particle-number conserving analysis for the systematics of high-K pair-broken bands in Hf and Lu isotopes ($170 \leqslant A \leqslant 178$)

Z. H. Zhang, Y. A. Lei,* and J. Y. Zeng

State Key Lab of Nuclear Physics and Technology, School of Physics, Peking University, Beijing 100871, People's Republic of China

(Received 8 May 2009; revised manuscript received 19 July 2009; published 18 September 2009)

Within the framework of the particle-number conserving (PNC) formalism, one-quasiparticle and low-lying high-K pair-broken (multiquasiparticle) bands systematically observed in Hf and Lu isotopes ($170 \leqslant A \leqslant 178$) are analyzed consistently. The PNC method deals with the cranked shell model with pairing interaction, in which the Pauli blocking effects are exactly accounted for, and the pairing interaction strength is determined by the experimental odd-even difference in binding energies. With an appropriate Nilsson level scheme that best fits the experimental bandhead energies of the one-quasiparticle bands, the experimental moments of inertia (MOIs) of these one-quasiparticle and multiquasiparticle bands (including configuration and frequency dependences, signature splitting, etc.) can be well reproduced without any additional free parameter. In most cases, the PNC formalism supports the configuration assignments in earlier works. the PNC calculation also reveals that the experimental systematics of low-lying high-K pair-broken bands in Hf and Lu isotopes are intimately related to the subshell effects near the Fermi surfaces of both protons and neutrons.

DOI: 10.1103/PhysRevC.80.034313 PACS number(s): 21.60.Cs, 23.20.Lv, 27.70.+q

I. INTRODUCTION

Low-lying high-K multiquasiparticle bands are systematically observed in the well-deformed rare-earth nuclei [1,2] because of the presence of several Nilsson orbitals with relatively high angular momentum projections Ω_i on the nuclear deformation axis near the Fermi surfaces of both neutrons and protons. The projection of the total nuclear angular momentum $K(=\sum_i \Omega_i)$ may be rather high. As a good approximation, K is a constant of motion and may serve as a convenient classification of the rotational bands depending on the corresponding intrinsic multiquasiparticle configurations. From the experimental level spacing of a rotational band, one can extract the associated moment of inertia (MOI) according to the rotational model. Considering that the bandhead excitation energies are relatively low, the Nilsson orbitals blocked by unpaired particles are close to the Fermi surface, and there may be only a few possible choices in the configuration assignment for a low-lying multiquasiparticle band when the spin and parity are known, particularly for the high-K bands. Usually the g_K-factor analysis for a multiquasiparticle band can provide an important argument to the choice of multiquasiparticle configuration. An independent confirmation of configuration assignment may be obtained by the MOI analysis of a multiquasiparticle band.

It is well known that the nuclear pairing correlation is very important in the low angular momentum region. As a consequence, the experimental MOI of the ground-state band (gsb) of an even-even nucleus is much smaller than that of the rigid-body estimation [3], and the MOIs of one-quasiparticle (1-qp) bands in odd-A nuclei are usually larger than those of the gsb's in adjacent even-even nuclei because of the blocking effects of unpaired nucleons [4]. The blocking effects of unpaired nucleons on MOIs of multiquasiparticle bands are even more important [5]. Usually the nuclear pairing interaction is treated by approximate methods such as the Bardeen-Cooper-Schrieffer (BCS) or Hartree-Fock-Bogoliubov (HFB) quasiparticle approaches. These approximations are standard in nuclear physics literature. Despite the great success of the quasiparticle approximation, both BCS and HFB methods suffer from serious problems [6,7]. One problem is the nonconservation of particle number and the occurrence of spurious states. Richardson [8] showed that an important class of low-lying excitations in nuclei cannot be described in standard BCS- or HFB-like theories. The remedy in terms of particle-number projection considerably complicates the calculation, yet with no improvement in the higher-excited spectrum of the pairing Hamiltonian [7]. Another well-known example is that in all self-consistent solutions to the HFB equation, a pairing collapse would occur if the nucleus were subjected to high-frequency rotation [9], but calculations with particle-number projection before variation have shown that the gap parameter $\Delta(\omega)$ decreases slowly with increasing rotational frequency ω and no sharp phase transition is found [10]. The most serious problem is the *blocking effect*, which is responsible for various odd-even differences in fundamental nuclear properties, e.g., nuclear binding energy and MOI. Rowe [11] pointed out that while the blocking effects are straightforward, they are very difficult to deal with in the BCS method, because they introduce different quasiparticle bases for different blocked levels; i.e., different pairing gap parameters must be introduced for different quasiparticle configurations. With the particle-number projection technique of Lipkin-Nogami, a discrete reduction in the gap parameter Δ with an increase of the seniority number (number of unpaired nucleons) was predicted [12]. The pairing reduction due to blocking effects was investigated with the particle-number conserving (PNC) method [13]. The details of the PNC formalism for the cranked shell model (CSM) with pairing interaction, $H_{\rm CSM} = H_0 + H_P$ ($H_0 = H_{\rm Nil} - \omega J_x$ being the one-body part and H_P the pairing correlation), were given

*yalei@pku.edu.cn

in Ref. [14]. In this article, we use the PNC formalism to systematically analyze the low-lying high-$K(K \geqslant 3)$ pair-broken bands in the well-deformed Hf and Lu isotopes, for which the experimental systematics is displayed in Fig. 1, and their configuration assignments are given in the caption. For convenience, some main PNC formulations used in the calculation are given in the Appendix. The key points of the PNC formalism are as follows:

(i) The particle number is conserved *from beginning to end* and the *blocking effects are exactly accounted for*.

(ii) A many-particle configuration (MPC) truncation (Fock-space truncation) is adopted in place of the conventional single-particle level (SPL) truncation in shell model calculations. As the number of important MPCs (with weights $>1\%$, say) involved in the low-lying excited states is very limited, it is not difficult to get sufficiently accurate solutions to the low-lying excited states. The stability of the final results with respect to the basis cutoff was illustrated in detail by Molique and Dudeck [7].

(iii) The effective pairing interaction strengths G_p (proton) and G_n (neutron) in the PNC calculation are determined by the experimental odd-even differences in nuclear binding energies. Once an appropriate Nilsson level scheme is adopted by best fitting the experimental bandhead energies of low-lying 1-qp bands in a given nucleus, no additional free parameter is involved in all PNC calculations, including MOI, bandhead energy, occupation probability, gap parameter, etc.

(iv) While the total number of nucleons is strictly conserved, the seniority is not a good quantum number because of the Coriolis antipairing interaction $-\omega J_x$. In general, the occupation probability n_μ for the cranked Nilsson orbital μ may change with increasing ω and may be quite different for various multiquasiparticle bands.

(v) The gap parameter Δ, *which is not a free parameter*, can be obtained in the PNC calculation. Usually the calculated Δ decreases with increasing rotational frequency ω and the ω dependence depends sensitively on the Coriolis response of Nilsson orbitals near the Fermi surface. Moreover, the calculated Δ and MOI are *automatically configuration dependent*, thus the PNC calculation of MOI with no free parameter can be a reliable argument for the configuration assignment of the multiquasiparticle band.

(vi) Though the projection of nuclear total angular momentum on the symmetry z axis of a spheroidal nucleus $K = \sum_i \Omega_i$ is a constant of motion, some forms of K mixing must exist to enable the K-forbidden transitions observed in rotational bands of axially symmetric nuclei [15,16]. In fact, because of the Coriolis interaction and $[J_x, J_z] \neq 0$, K varies with increasing ω. However, considering $[J_x, J_z^2] = 0$, in the PNC calculation, each cranked MPC (CMPC) is chosen as a simultaneous eigenstate of (H_0, J_z^2) (see Appendix).

In Sec. II, the systematics of the low-lying high-$K(K \geqslant 3)$ pair-broken states (2-qp bands in even-even Hf isotopes and related 3-qp bands in odd-A Hf and Lu isotopes) are analyzed. For example, low-lying proton pair-broken bands $K^\pi = 6^+(\pi 7/2^+[404] \otimes \pi 5/2^+[402])$, $8^-(\pi 7/2^+[404] \otimes \pi \mathbf{9/2^-[514]})$ (the bold face numbers indicate the high-j intruder orbitals), and neutron pair-broken bands $K^\pi = 4^-(\nu \mathbf{7/2^+[633]} \otimes \nu 1/2^-[521])$, $6^-(\nu \mathbf{7/2^+[633]} \otimes \nu 5/2^-[512])$, $3^+(\nu 1/2^-[521] \otimes \nu 5/2^-[512])$, $8^-(\nu 7/2^-[514] \otimes \nu \mathbf{9/2^+[624]})$, etc., were consistently observed in the even-even Hf isotopes (see Figs. 1, 7, 8, 11) [2,17–22]. The related proton pair-broken (3-qp) bands $K^\pi = 19/2^+(\pi^2 6^+ \otimes \nu \mathbf{7/2^+[633]})$ and $23/2^-(\pi^2 8^- \otimes \nu \mathbf{7/2^+[633]})$ were observed in the adjacent odd-A Hf isotopes [18,23–28]. The related neutron pair-broken bands $K^\pi = 15/2^-(\pi 7/2^+[404] \otimes \nu^2 4^-)$, $23/2^-(\pi 7/2^+[404] \otimes \nu^2 8^-)$, $25/2^+(\mathbf{9/2^-[514]} \otimes \nu^2 8^-)$, etc., were also established in odd-A Lu isotopes (see Figs. 8 and 11) [29–32]. Using systematics arguments, the configuration assignment of these pair-broken bands has been discussed in Refs. [2,20]. Careful examination will show that the systematics of low-lying high-K ($\geqslant 3$) pair-broken bands in Hf and Lu isotopes are intimately related to the *subshell effects* of both protons and neutrons (see Fig. 2).

Some low-lying high-K bands in the lighter $^{172-175}$Hf isotopes have been analyzed in the PNC formalism [5] using the Nilsson level scheme of Lund systematics [33,34]. First, though the Lund systematics is greatly successful in predicting the ground-state spins of well-deformed rare-earth nuclei, deviations of the experimental bandhead energies of 1-qp bands from the prediction by the Lund systematics have been noted (e.g., see Ref. [35]). To improve the calculations of the bandhead energies, MOIs for 1-qp and pair-broken bands, and their configuration assignments, in this paper, the Nilsson parameters (κ, μ) of Lund systematics [33] are slightly adjusted to reproduce the correct experimental bandhead energies of 1-qp bands. For the details, see the captions of Figs. 3, 4, and 9. Second, to illustrate the systematics of low-lying high-K bands, the large amount of experimental 1-qp and high-K pair-broken bands in Hf and Lu isotopes ($170 \leqslant A \leqslant 178$) are consistently analyzed.

In Sec. III, we give a consistent PNC analysis for the low-lying bands in Hf and Lu nuclei ($170 \leqslant A \leqslant 176$), including the bandhead energy and MOI. Because of the subshell ($N = 104$) effect, differences are noted in the systematics of the low-lying high-K pair-broken bands between the lighter ($N \leqslant 104$) and the heavier ($N > 104$) Hf and Lu isotopes, so the low-lying bands in ^{177,178}Hf and ^{177}Lu are discussed in Sec. IV. In Sec. V, other multiquasiparticle bands in Hf and Lu isotopes are addressed. A summary is given in Sec. VI. For convenience, some PNC essentials are given in the Appendix.

II. SYSTEMATICS OF LOW-LYING PAIR-BROKEN STATES IN Hf AND Lu ISOTOPES AND SUBSHELL EFFECTS

The schematic graphs of subshells near the Fermi surface of protons and neutrons for the well-deformed Lu and Hf isotopes are shown in Figs. 2(a) and 2(b). We see that (1) near the proton Fermi surface of well-deformed rare-earth nuclei, there exist two small gaps at $Z = 70$ and $Z = 76$, and the

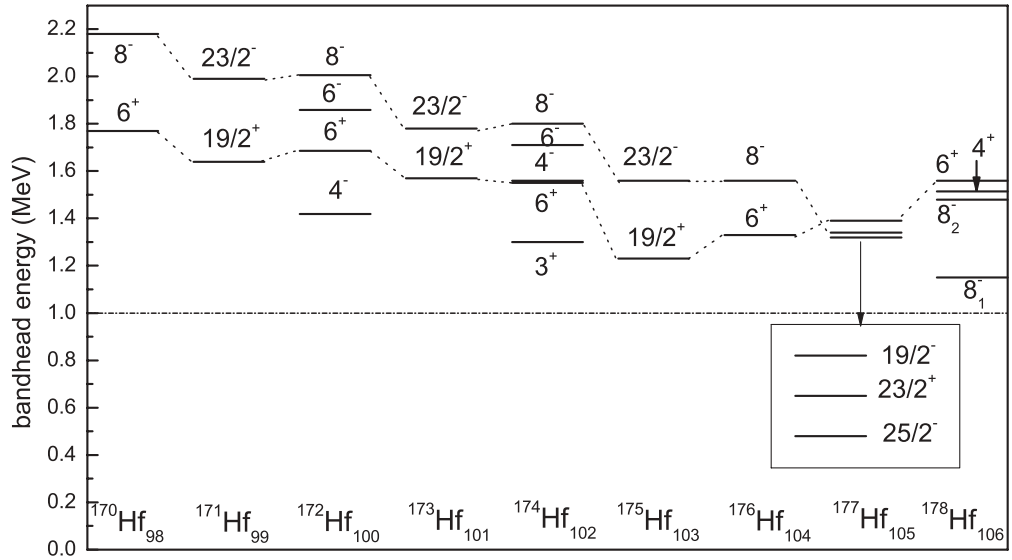

FIG. 1. Systematics of experimental low-lying high-K ($\geqslant 3$) pair-broken bands in Hf and Lu isotopes [2,17–32]. The dominant configurations of the pair-broken bands in even-even Hf isotopes were assigned as $K^\pi = 6^+(\pi 7/2^+[404] \otimes \pi 5/2^+[402])$, $8^-(\pi 7/2^+[404] \otimes \pi \mathbf{9/2^-[514]})$, $4^-(\nu \mathbf{7/2^+[633]} \otimes \nu 1/2^-[521])$, $6^-(\nu \mathbf{7/2^+[633]} \otimes \nu 5/2^-[512])$, $3^+(\nu 1/2^-[521] \otimes \nu 5/2^-[512])$, etc. The configuration components may be different for the bands in lighter ($N \leqslant 104$) and heavier ($N > 104$) nuclei. For the related proton pair-broken (3-qp) bands $K^\pi = 19/2^+(\pi^2 6^+ \otimes \nu \mathbf{7/2^+[633]})$ and $23/2^-(\pi^2 8^- \otimes \nu \mathbf{7/2^+[633]})$ in ^{171,173,175}Hf, the bandhead energies of one-quasineutron bands $K^\pi = 7/2^+$ and $9/2^-$ have been subtracted (see Fig. 3). Similarly, for the $K^\pi = 23/2^+(\pi^2 8^- \otimes \nu 7/2^-[514])$, $25/2^-(\pi^2 8^- \otimes \nu \mathbf{9/2^+[624]})$, and $19/2^-(\pi^2 6^+ \otimes \nu 7/2^-[514])$ bands in ^{177}Hf, the bandhead energies of three low-lying one-quasineutron bands $\nu 7/2^-[514]$, $\nu \mathbf{9/2^+[624]}$, and $\nu 5/2^-[512]$ (see Fig. 9) have been subtracted, respectively. As there is no even-even isotope for Lu, the systematics of the low-lying neutron pair-broken bands in Lu isotopes are not as obvious as in Hf ones. The neutron pair-broken band $K^\pi = 15/2^-(\pi 7/2^+[404] \otimes \nu^2 4^-)$ at 1241 keV in ^{171}Lu is analogous to the $K^\pi = 4^-$ band at 1418 keV in ^{172}Hf, except for a spectator proton $\pi 7/2^+[404]$ (see Fig. 8). Similarly, the $K^\pi = 19/2^+$ state at 1391 keV in ^{175}Lu is analogous to the $K^\pi = 6^+$ state at 1333 keV in ^{176}Hf. The neutron pair-broken state $K^\pi = 23/2^-$ at 970 keV and $K^\pi = 25/2^+$ at 1325 keV in ^{177}Lu are considered as $\pi 7/2^+[404] \otimes \nu^2 8^-(7/2^-[514] \otimes \mathbf{9/2^+[624]})$ and $\pi \mathbf{9/2^-[514]} \otimes \nu^2 8^-$, respectively (see Fig. 11).

Nilsson orbitals between the two small gaps, $\pi 7/2^+[404]$, $\pi 5/2^+[402]$, and $\pi \mathbf{9/2^-[514]}$, form a subshell [Fig. 2(a)]; and (2) near the neutron Fermi surface, there exist two small gaps at $N = 98$ and $N = 104$, and the neutron orbitals $\nu \mathbf{7/2^+[633]}$, $\nu 1/2^-[521]$, and $\nu 5/2^-[512]$ form a subshell [Fig. 2(b)]. This explains the experimental systematics of low-lying pair-broken states of Hf and Lu isotopes.

According to Gallagher [36], for the pair-broken states, the spin singlet coupling is energetically favored. In fact, almost all the observed proton (neutron) pair-broken states in Fig. 1 are spin singlets, i.e.,

$$\pi^2 6^+(7/2^+[404] \otimes 5/2^+[402]),$$
$$\pi^2 8^-(7/2^+[404] \otimes \mathbf{9/2^-[514]}),$$
$$\nu^2 4^-(\mathbf{7/2^+[633]} \otimes 1/2^-[521]),$$
$$\nu^2 3^+(1/2^-[521] \otimes 5/2^-[512]),$$
$$\nu^2 6^+(5/2^-[512] \otimes 7/2^-[514]),$$
$$\nu^2 8^-(7/2^-[514] \otimes \mathbf{9/2^+[624]}).$$

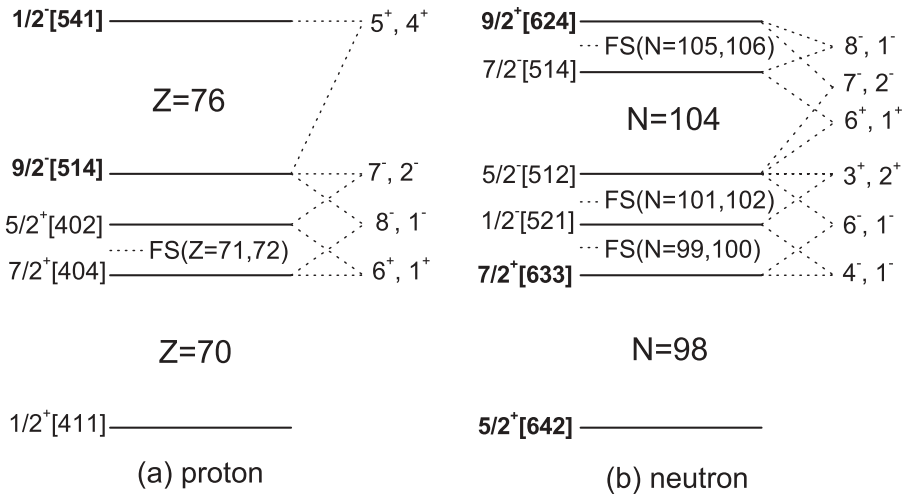

FIG. 2. Schematic graph of subshells near the Fermi surface of the well-deformed Hf and Lu isotopes (see Figs. 3, 4, 9).

The low-lying $\nu^2 6^-(\mathbf{7/2^+[633]} \otimes 5/2^-[512])$ is an exception, which is a spin triplet. However, it should be noted that for all the well-deformed even-even Hf nuclei, low-lying *low-K* pair-broken $K^\pi = |\Omega_1 - \Omega_2|^\pi = 1^-$ (triplet, or singlet) states (see Fig. 2) are common, of which coherent superposition is usually considered as an octuple vibrational excitation, where the Gallagher rule fails. In singlets, the intrinsic-spin g_K factor cancels, neutrons yield $g_K \sim 0$, protons yield $g_K \sim 1$ [18], which is very useful in configuration assignment.

A. Low-lying high-K proton pair-broken states

For the even-even Hf ($Z = 72$) isotopes, the lowest lying proton pair-broken (two-quasiproton) state is $\pi^2 6^+(7/2^+[404] \otimes 5/2^+[402])$ [Fig. 2(a)]. The experimental low-lying $K^\pi = 6^+$ states in ^{170,172,174}Hf were considered as of a rather pure proton configuration $\pi^2 6^+$ [2,17–20]; but with increasing neutron number ($N \geqslant 104$), the dominant $\pi^2 6^+$ excitation may slightly mix with the low-lying neutron pair-broken (two-quasineutron) configuration $\nu^2 6^+(5/2^-[512] \otimes 7/2^-[514])$ [19,21,22,25,28] [see Fig. 2(b)]. The PNC calculations for MOIs confirm this statement (see Fig. 7). The estimate of Dracoulis [23,26] showed that the 6^+ state in ^{176}Hf ($N = 104$) has a $\nu^2 6^+$ admixture of about 40%.

The dominant configuration of experimental low-lying $K^\pi = 8^-$ bands in ^{170,172,174,176}Hf was assigned as the low-lying $\pi^2 8^-(7/2^+[404] \otimes \mathbf{9/2^-[514]})$ [Fig. 2(a)] [2,17–22,28]. The magnitude of the neutron configuration $\nu^2 8^-$ is expected to be less for the $K^\pi = 8^-$ state than for the $K^\pi = 6^+$ state [26]. This is because the $\nu^2 8^-(7/2^-[514] \otimes \mathbf{9/2^+[624]})$ excitation is relatively high for $N \leqslant 104$ Hf isotopes [see Fig. 2(b)]. The PNC calculations for MOIs confirm this statement (see Sec. III and Fig. 7). The experimental two low-lying $K^\pi = 8^-$ states in ^{178}Hf ($N = 106$) (8_1^- at 1147 keV and 8_2^- at 1479 keV) may be considered as admixtures of the lowest lying neutron pair-broken state $\nu^2 8^-$ and the low-lying proton pair-broken state $\pi^2 8^-$ [21,22,28].

The experimental low-lying pair-broken (3-qp) $K^\pi = 19/2^+$ states in the odd-A Hf isotopes (at 1645 keV in ^{171}Hf, 1670 keV in ^{173}Hf, and 1433 keV in ^{175}Hf) are analogous to the $K^\pi = 6^+$ states in ^{170,172,174}Hf, respectively, except for a spectator neutron $\nu\mathbf{7/2^+[633]}$ [18,23–26]. Their decay properties support the configuration assignment $\pi^2 6^+ \otimes \nu\mathbf{7/2^+[633]}$. Our PNC calculation for MOIs also favors this assignment (see Fig. 7). Similarly, the low-lying pair-broken (3-qp) bands $K^\pi = 23/2^-$ observed in ^{171}Hf (1986 keV), ^{173}Hf (1981 keV), and ^{175}Hf (1766 keV) are analogous to the $K^\pi = 8^-$ bands in ^{170}Hf, ^{172}Hf, and ^{174}Hf, respectively, except for a spectator neutron $\nu\mathbf{7/2^+[633]}$. In Fig. 1, the spectator neutron $\nu\mathbf{7/2^+[633]}$ excitation energy has been subtracted from the bandhead energies of the $K^\pi = 19/2^+$ and $K^\pi = 23/2^-$ bands in ^{171,173,175}Hf. It is noted that the systematics of the bandhead energies of the pair-broken bands $K^\pi = 6^+(8^-)$ in the even-even Hf isotopes are quite similar to those of the analogous pair-broken bands $K^\pi = 19/2^+(23/2^-)$ in the neighboring odd-A Hf isotopes.

For ^{177}Hf ($N = 105$), the gsb is $\nu 7/2^-[514]$, and the first excited band is $\nu\mathbf{9/2^+[624]}$. The dominant configurations of the low-lying $K^\pi = 19/2^-$ state at 1343 keV and $K^\pi = 23/2^+$ state at 1316 keV were expected to be $\pi^2 6^+ \otimes \nu 7/2^-[514]$ and $\pi^2 8^- \otimes \nu 7/2^-[514]$, respectively [27]. The next higher pair-broken band $K^\pi = 25/2^-$ state at 1713 keV was expected to be $\pi^2 8^- \otimes \nu\mathbf{9/2^+[624]}$. Unlike the $K^\pi = 8_1^-$ and $K^\pi = 8_2^-$ in ^{178}Hf, the $\nu^2 8^-(7/2^-[514] \otimes \mathbf{9/2^+[624]})$ configuration is ruled out for the $K^\pi = 23/2^+$ and $K^\pi = 25/2^-$ bands in ^{177}Hf by the Pauli principle [27]. It is interesting to note that $[E(25/2^-) - E(9/2^+)] = 1392$ keV is very close to $[E(23/2^+) - E(7/2^-)] = 1316$ keV. The small difference may come from the small residual neutron-proton interaction.

B. Low-lying high-K neutron pair-broken states

For ^{170}Hf ($N = 98$), the neutron Fermi level is located in the neutron small gap at $N = 98$, and the subshell ($\nu\mathbf{7/2^+[633]}$, $\nu 1/2^-[521]$, $\nu 5/2^-[512]$) is closed [Fig. 2(b)], thus it is understandable that no low-lying ($E < 2.2$ MeV) excited high-K neutron pair-broken band is observed.

For ^{172}Hf ($N = 100$), the expected lowest lying high-K neutron pair-broken state is $K^\pi = 4^-(\nu\mathbf{7/2^+[633]} \otimes \nu 1/2^-[521])$ [Fig. 2(b)], which was observed at 1416 keV [17]. The related neutron pair-broken $K^\pi = 15/2^-$ state at 1241 keV in ^{171}Lu was assigned to be of $\pi 7/2^+[404] \otimes \nu^2 4^-$ [29,30], analogous to the $K^\pi = 4^-$ state in ^{172}Hf, except for a spectator proton $\pi 7/2^+[404]$. The next higher high-K neutron pair-broken state in ^{172}Hf is expected to be $K^\pi = 6^-(\nu\mathbf{7/2^+[633]} \otimes \nu 5/2^-[512])$, which was observed at 1858 keV [17]. Another expected low-lying high-K pair-broken state $K^\pi = 3^+(\nu 1/2^-[521] \otimes \nu 5/2^-[512])$ [see Fig. 2(b)] has not yet been identified in ^{172}Hf.

For ^{174}Hf ($N = 102$), the expected lowest lying neutron pair-broken state is $\nu^2 3^+(1/2^-[521] \otimes 5/2^-[512])$ [Fig. 2(b)], which was assigned as the observed pair-broken state $K^\pi = 3^+$ at 1304 keV [18]. The other two low-lying high-K neutron pair-broken bands $K^\pi = 4^-$ at 1562 keV and $K^\pi = 6^-$ at 1713 keV were assigned as $\nu^2 4^-(\mathbf{7/2^+[633]} \otimes 1/2^-[521])$ and $\nu^2 6^-(\mathbf{7/2^+[633]} \otimes 5/2^-[512])$, respectively.

For ^{176}Hf ($N = 104$), the neutron subshell is closed [Fig. 2(b)] and the expected low-lying high-K neutron pair-broken states are $\nu^2 6^+(5/2^-[512] \otimes 7/2^-[514])$ and $\nu^2 7^-(5/2^-[512] \otimes \mathbf{9/2^+[624]})$. The experimental $K^\pi = 6^+$ state at 1333 keV in ^{176}Hf was considered as an mixture of $\pi^2 6^+(7/2^+[404] \otimes 5/2^+[402])$ and $\nu^2 6^+(5/2^-[512] \otimes 7/2^-[514])$ [19,23,26]. The observed $K^\pi = 19/2^+$ state at 1391 keV in ^{175}Lu was considered as the lowest lying neutron pair-broken state $\pi 7/2^+[404] \otimes \nu^2 6^+$ [Fig. 2(a)] [31], which is analogous to the $K^\pi = 6^+$ state in ^{176}Hf except for the spectator proton $\pi 7/2^+[404]$. The situation of ^{177}Lu ($N = 105$) is a little different. The low-lying pair-broken states $K^\pi = 23/2^-$ at 970 keV and $K^\pi = 25/2^+$ at 1325 keV were considered as the pure neutron pair-broken states $\pi 7/2^+[404] \otimes \nu^2 8^-$ and $\pi\mathbf{9/2^-[514]} \otimes \nu^2 8^-$, respectively, because the configuration $\pi^2 8^-(7/2^+[404] \otimes \mathbf{9/2^-[514]})$ violates the Pauli principle [32].

Finally, Fig. 2 shows that while low-lying high-K pair-broken states $K = |\Omega_1 + \Omega_2| > 3$ are very limited for a given nucleus, there exist a large number of *low-K* pair-broken states

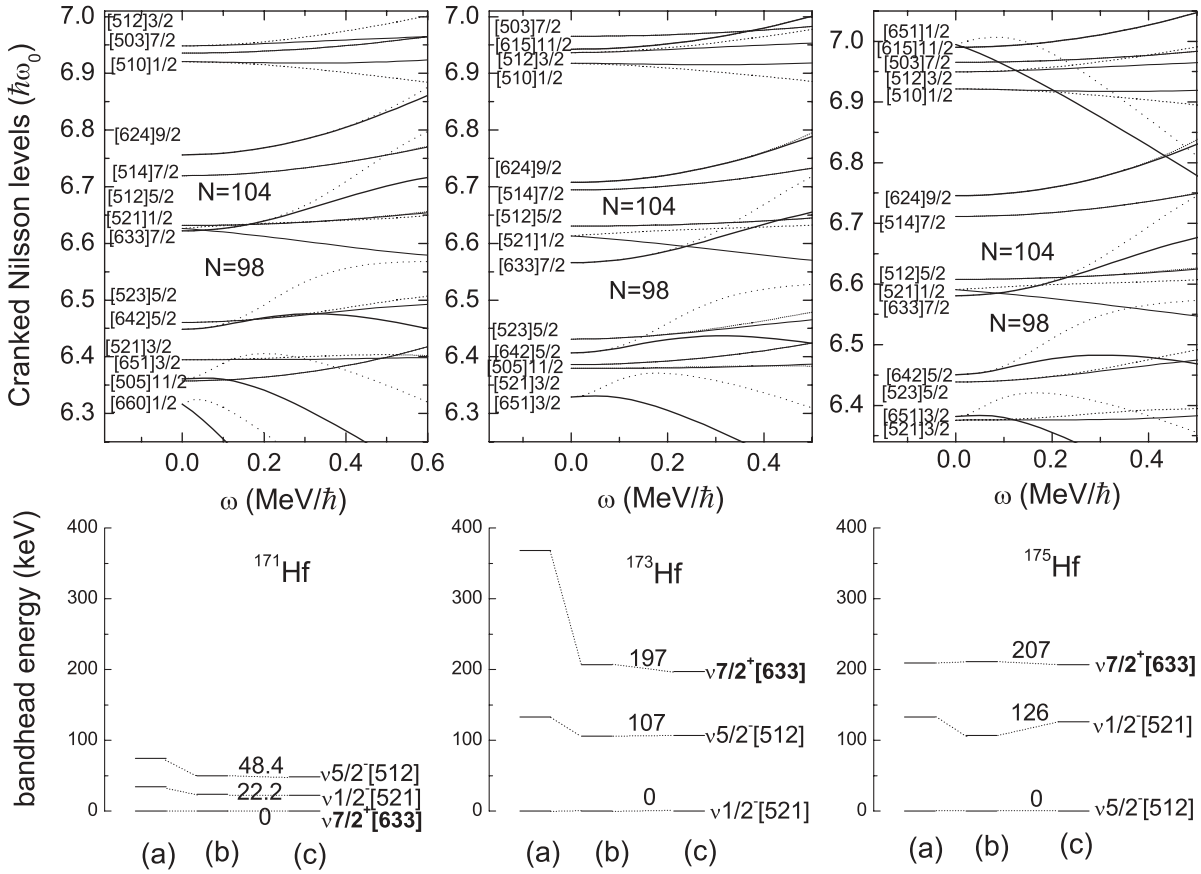

FIG. 3. Neutron cranked Nilsson orbitals near the Fermi surface of ^{171,173,175}Hf. The deformation parameters $(\varepsilon_2, \varepsilon_4)$ are taken from the Lund systematics [33], $(\varepsilon_2, \varepsilon_4) = (0.2495, 0.0185)$, $(0.256, 0.0285)$, $(0.257, 0.0385)$ for ^{171,173,175}Hf, respectively. The Nilsson parameters κ and μ (Lund systematics) are slightly adjusted to reproduce the bandhead energies of low-lying one-quasineutron bands of ^{171,173,175}Hf (see the lower part). For ^{171}Hf, $\kappa_5 = 0.0636$, $\kappa_6 = 0.0636$, $\mu_5 = 0.413$, and $\mu_6 = 0.413$, and $1/2^-[521]$ is shifted further upward by $0.028\,\hbar\omega_0$, $\mathbf{7/2^+[633]}$ upward by $0.040\,\hbar\omega_0$. For ^{173}Hf, $\kappa_5 = 0.0610$, $\kappa_6 = 0.0636$, $\mu_5 = 0.440$, and $\mu_6 = 0.451$, and $1/2^-[521]$ is shifted further upward by $0.030\,\hbar\omega_0$, $\mathbf{7/2^+[633]}$ upward by $0.035\hbar\omega_0$. For ^{175}Hf, $\kappa_5 = 0.0673$, $\kappa_6 = 0.0625$, $\mu_5 = 0.408$, and $\mu_6 = 0.408$, and $5/2^-[512]$ is shifted further downward by $0.010\hbar\omega_0$, $\mathbf{7/2^+[633]}$ upward by $0.012\hbar\omega_0$. (a) Simple shell model calculation of the bandhead energies using the above Nilsson level scheme. (b) PNC calculation for the bandhead energies. The neutron effective pairing interaction strength G_n is determined by the experimental odd-even difference in binding energies, $G_n = 0.46$ MeV for ^{171}Hf, $G_n = 0.34$ MeV for ^{173}Hf, and $G_n = 0.30$ MeV for ^{175}Hf. (c) Experimental results.

$(K = |\Omega_1 - \Omega_2| = 1, 2)$. For example, the widely observed low-lying $K^\pi = 2^+$ γ-vibrational bands in well-deformed nuclei may be described as coherent superpositions of a large number of neutron and proton pair-broken configurations with $K^\pi = 2^+$, in which the residual proton-neutron interaction should be taken into account.

III. PNC ANALYSIS FOR LOW-LYING BANDS IN Hf AND Lu ISOTOPES ($171 \leqslant A \leqslant 176$)

A. Low-lying 1-qp bands in ^{171,173,175}Hf and ^{171,173,175}Lu

The cranked neutron levels near the Fermi surface of ^{171,173,175}Hf are given in Fig. 3. The deformation parameters $(\varepsilon_2, \varepsilon_4)$ are taken from the Lund systematics [33]. To reproduce the experimental bandhead energies of 1-qp bands, the Nilsson parameters (κ, μ) of Lund systematics are slightly adjusted. A small adjustment in μ may cause the Nilsson level relative position change in the same N shell, and a small variation in κ may lead to the relative position change of neighboring N shells. The details of Nilsson level changes are given in the caption of Fig. 3.

Using these cranked Nilsson neutron level schemes (Fig. 3), the simple shell model calculations (pairing interaction missing) of the bandhead energies of one-quasineutron bands in ^{171,173,175}Hf are also given in the lower part of Fig. 3, column (a). Figure 3(b) shows the PNC calculated bandhead energies of the 1-qp bands, in which the neutron effective pairing interaction strength is determined by the experimental odd-even differences in binding energies (see the caption of Fig. 3). The effective pairing interaction strength thus determined is used to perform *all PNC calculations*, including the MOIs of the 1-qp (Fig. 5) and pair-broken (multiquasiparticle) bands (Fig. 7), etc. Thus, *no free parameter* is involved in the calculation. The experimental bandhead energies of 1-qp bands in ^{171,173,175}Hf are shown in Fig. 3(c). Figure 4 is the

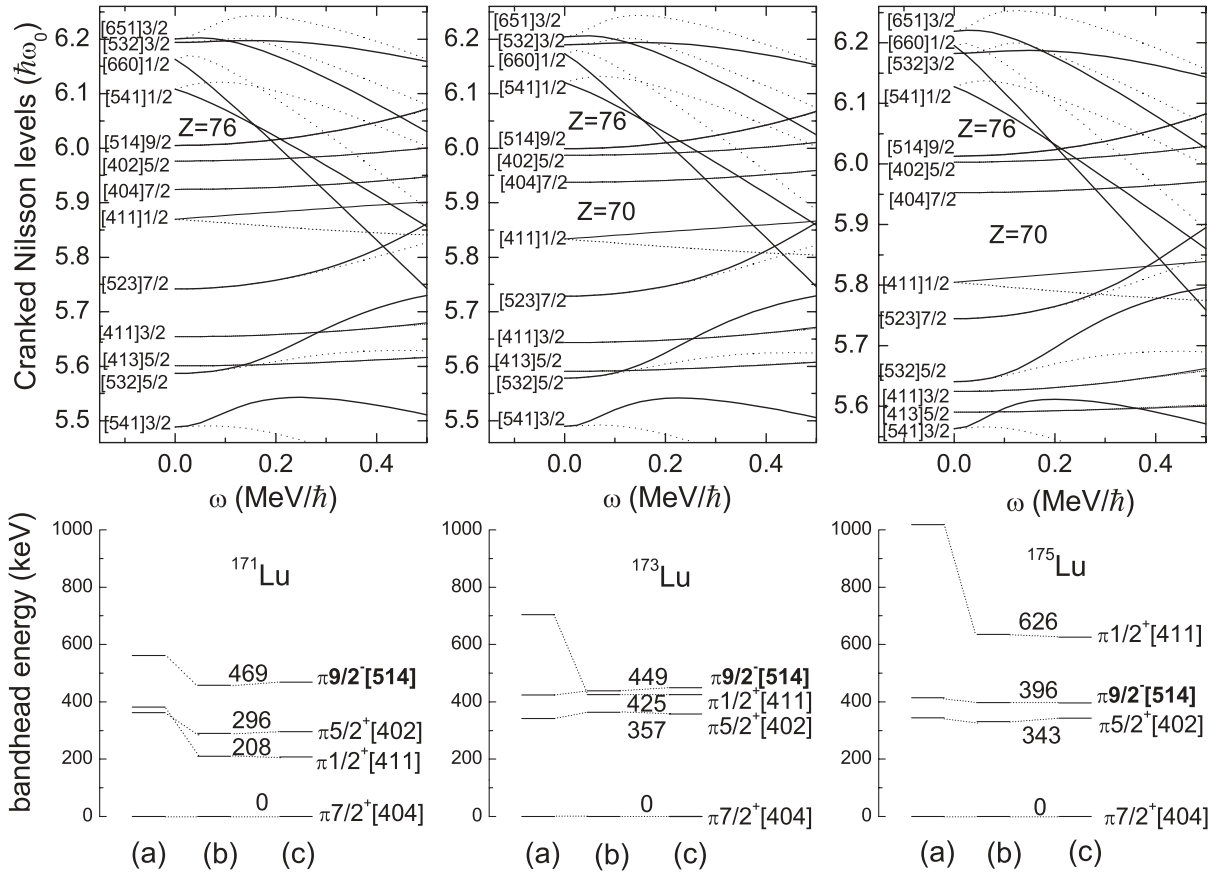

FIG. 4. Same as Fig. 3, but for the proton cranked Nilsson orbitals near the Fermi surface of ^{171,173,175}Lu. The deformation parameters $(\varepsilon_2, \varepsilon_4)$ are taken from the Lund systematics [33], $(\varepsilon_2, \varepsilon_4) = (0.2595, 0.024)$, $(0.2635, 0.035)$, $(0.261, 0.0455)$ for ^{171,173,175}Lu, respectively. The Nilsson parameters κ and μ (Lund systematics) are slightly adjusted to reproduce the bandhead energies of the low-lying one-quasiproton bands of ^{171,173,175}Lu, shown in the lower part. For ^{171}Lu, $\kappa_4 = 0.0615$, $\kappa_5 = 0.0650$, $\mu_4 = 0.604$, $\mu_5 = 0.601$, and $\mathbf{9/2^-[514]}$ is further shifted upward by $0.046\,\hbar\omega_0$, $1/2^+[411]$ upward by $0.040\,\hbar\omega_0$, $5/2^+[402]$ downward by $0.024\,\hbar\omega_0$. For ^{173}Lu, $\kappa_4 = 0.0615$, $\kappa_5 = 0.0650$, $\mu_4 = 0.601$, $\mu_5 = 0.599$, and $\mathbf{9/2^-[514]}$ is further shifted upward by $0.046\,\hbar\omega_0$, $1/2^+[411]$ upward by $0.015\,\hbar\omega_0$, $5/2^+[402]$ downward by $0.024\,\hbar\omega_0$. For ^{175}Lu, $\kappa_4 = 0.0620$, $\kappa_5 = 0.0570$, $\mu_4 = 0.580$, $\mu_5 = 0.607$, and $1/2^+[411]$ is further shifted upward by $0.005\,\hbar\omega_0$, $\mathbf{7/2^-[523]}$ downward by $0.04\hbar\omega_0$. The proton effective pairing interaction strength $G_p = 0.35$ MeV for ^{171}Lu, $G_p = 0.33$ MeV for ^{173}Lu, and $G_p = 0.34$ MeV for ^{175}Lu. (a), (b), (c) are the same as in Fig. 3.

same as Fig. 3, but for the cranked proton Nilsson levels and bandhead energies of one-quasiproton bands of ^{171,173,175}Lu. The experimental bandhead energies of these 1-qp bands are well reproduced by PNC calculations.

The experimental and calculated MOIs of low-lying one-quasineutron bands in ^{171,173,175}Hf and one-quasiproton bands in ^{171,173,175}Lu are shown in Figs. 5 and 6, respectively. The experimental MOIs are denoted by solid ■ ($\alpha = 1/2$) and open □ ($\alpha = -1/2$) squares, respectively. The calculated MOIs by the PNC method are solid ($\alpha = 1/2$) and dotted ($\alpha = -1/2$) lines, respectively. For comparison, the experimental MOIs of the reference bands ($K^\pi = 0^+$, $\alpha = 0$, gsb of the neighboring even-even nucleus, i.e., qp-vacuum band) are also shown by +. The experimental kinematic MOI for each band is separately extracted by the intraband transition energies $E_\gamma(I+1 \to I-1)$ for each signature sequence within a rotational band ($I = \alpha \bmod 2$), $I \geqslant K$, as follows:

$$\frac{J^{(1)}(I)}{\hbar^2} = \frac{2I+1}{E_\gamma(I+1 \to I-1)}. \tag{1}$$

The dependence of the rotational frequency ω and nuclear angular momentum I is

$$\hbar\omega(I) = \frac{E_\gamma(I+1 \to I-1)}{I_x(I+1) - I_x(I-1)}, \tag{2}$$

where $I_x(I) = \sqrt{(I+1/2)^2 - K^2}$, and K is the projection of the nuclear total angular momentum along the symmetry z axis, which is usually considered as a rough good quantum number in each band.

It is seen that the large amount of experimental data of MOIs of these 1-qp bands are well reproduced by the PNC calculations with no free parameter.

Both the experimental and calculated MOIs of the one-quasineutron band $\nu\mathbf{7/2^+[633]}$ are much larger than that of the reference band at low ω (see Fig. 5). This is because the high-$j(i_{13/2})$ intruder orbital $\nu\mathbf{7/2^+[633]}$ is blocked, which has a large antipairing Coriolis response. However with increasing ω, the odd-even difference in MOIs becomes smaller and smaller and finally vanishes.

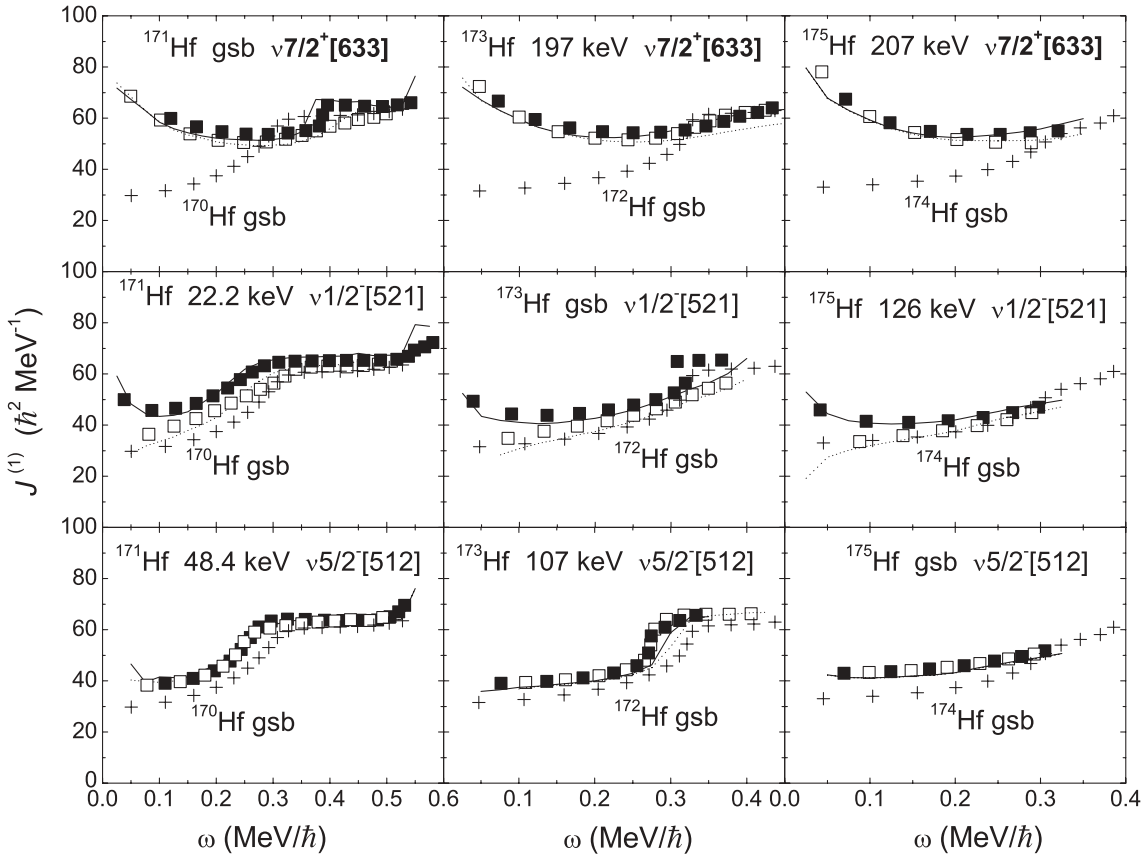

FIG. 5. MOIs of the low-lying 1-qp bands in ^{171,173,175}Hf. The experimental MOIs are denoted by ■ ($\alpha = 1/2$) and □ ($\alpha = -1/2$). The calculated MOIs by the PNC method are denoted by solid lines ($\alpha = 1/2$) and dotted lines ($\alpha = -1/2$). The experimental MOIs of the reference band ($K^\pi = 0^+$, $\alpha = 0$, gsb, i.e., the quasivacuum band) are denoted by +.

In contrast, for the one-quasiproton bands $\pi 7/2^+[404]$ and $\pi 5/2^+[402]$, the MOIs are almost equal to that of the reference band (see Fig. 6). This is because the blocked deformation-aligned orbitals $\pi 7/2^+[404]\,(g_{7/2})$ and $\pi 5/2^+[402]\,(d_{5/2})$ have a negligibly small Coriolis response. This is the PNC microscopic demonstration of the "identical bands" observed in a lot of rotational bands in the rare-earth nuclei [37]. The neutron $\nu 5/2^-[512]\,(h_{9/2})$ and proton $\pi \mathbf{9/2^-[514]}\,(h_{11/2})$ bands are the intermediate cases. Though the proton Nilsson orbital $\pi \mathbf{9/2^-[514]}\,(h_{11/2})$ is a high-j intruder orbital, it is a high-Ω (deformation-aligned) state having only a small Coriolis response, so we can understand the observed small odd-even differences in MOIs.

An obvious signature splitting in MOIs is observed for the one-quasineutron band $\nu \mathbf{7/2^+[633]}$ at $\hbar\omega > 0.15$ MeV, which can be understood from the behavior of the cranked Nilsson orbital $\nu \mathbf{7/2^+[633]}$ (see Fig. 3). Obvious signature splittings near the bandhead are observed in the $K = 1/2$ bands ($\pi 1/2^+[411]$) in ^{171,173,175}Lu and ($\nu 1/2^-[521]$) in ^{171,173,175}Hf, which can be understood from the non-zero Coriolis matrix element $(\Omega = 1/2|j_x|\Omega = -1/2) \neq 0$. However, with increasing ω, the signature splitting gradually decreases.

The experimental MOI of the $K^\pi = 1/2^+$ band in ^{171}Lu is not reproduced well by the PNC calculation for the configuration $\pi 1/2^+[411]$, particularly the early unbending, which is not yet well explained [29]. In addition, the high-spin behavior of the gsb $\nu 1/2^-[521]$ in ^{173}Hf (backbending at $\hbar\omega \sim 0.30$ MeV of the $\alpha = 1/2$ sequence, Fig. 5) is not well understood yet, though larger core deformation might play a role [25].

B. Low-lying pair-broken bands in Hf and Lu isotopes ($171 \leqslant A \leqslant 176$)

Now we analyze the MOIs of low-lying high-K ($K \geqslant 3$) pair-broken bands in Hf and Lu isotopes ($171 \leqslant A \leqslant 176$). The MOIs are calculated by the PNC method using *the same Nilsson level scheme as in Figs. 3 and 4* and *the same pairing interaction strength; no additional free parameters are involved in the calculations*. For example, for MOIs of pair-broken bands of ^{174}Hf, the cranked proton (neutron) Nilsson level scheme and the proton (neutron) pairing interaction strength G_p (G_n) are the same as ^{173}Lu (^{173}Hf) (see Figs. 3 and 4). It is found that the calculated MOI of a pair-broken band depends sensitively on the assigned configuration. Once an appropriate configuration is adopted, the experimental MOI can be well reproduced by PNC calculations (see Fig. 7). It is well known that the g_K-factor analysis is very helpful in the configuration assignment of a multiquasiparticle band. The PNC calculation of MOI with no free parameter can provide another independent and reliable argument for the

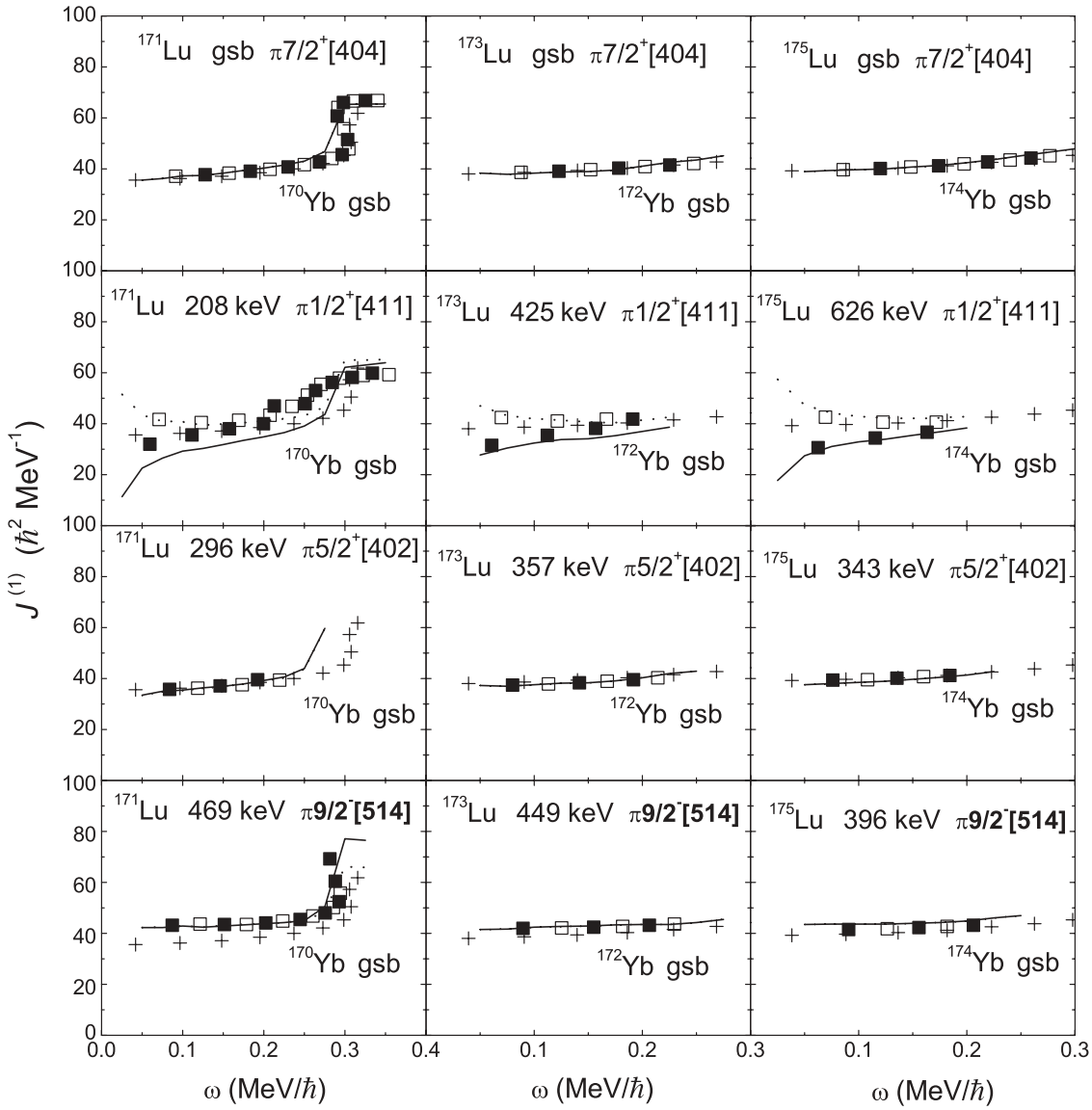

FIG. 6. Same as Fig. 5, but for the MOIs of the low-lying 1-qp bands in ^{171,173,175}Lu. No significant signature splitting is observed at low frequencies except for the $\pi 1/2^+[411]$ band.

configuration assignment of a low-lying high-K pair-broken band.

1. Low-lying high-K proton pair-broken bands

The MOIs of low-lying high-K proton pair-broken bands are shown in Fig. 7. For the $K^\pi = 6^+$ band at 1686 keV in ^{172}Hf and $K^\pi = 6^+$ band at 1549 keV in ^{174}Hf, the calculated MOIs using the expected lowest lying proton pair-broken configuration $\pi^2 6^+(7/2^+[404] \otimes 5/2^+[402])$ [see Fig. 2(a)] agree very well with the experimental results. However, as the neutron Fermi surface rises with the addition of extra neutrons, the neutron pair-broken excitation $\nu^2 6^+(5/2^-[512] \otimes 7/2^-[514])$ gradually decreases, particularly for $N \geqslant 104$ [see Fig. 2(b)], which may be mixed with the low-lying $\pi^2 6^+$ configuration. The PNC calculated MOIs of ^{176}Hf for both the $\pi^2 6^+$ and $\nu^2 6^+$ configurations are shown in Fig. 7. It is found that the experimental MOI of the $K^\pi = 6^+$ band at 1333 keV in ^{176}Hf cannot be well reproduced by the PNC calculations for the *pure* $\pi^2 6^+$ or $\nu^2 6^+$ configuration, which supports the statement that the $K^\pi = 6^+$ band in ^{176}Hf is an *admixture* of $\pi^2 6^+$ and $\nu^2 6^+$ [23,26]. However, it is seen that the experimental MOI of $K^\pi = 6^+$ band in ^{176}Hf is closer to the PNC calculation using the $\pi^2 6^+$ configuration than that using the $\nu^2 6^+$ configuration, so the dominant configuration should be $\pi^2 6^+$, but a certain amount of $\nu^2 6^+$ admixture should not be ignored. In addition, the PNC calculations for the bandhead energies E also support the above statement; i.e., for the $K^\pi = 6^+$ band,

$$E_{\rm cal} = 1633, 1652, 1377 \text{ keV} \quad \text{for} \quad {}^{172,174,176}\text{Hf},$$
$$E_{\rm exp} = 1686, 1549, 1333 \text{ keV} \quad \text{for} \quad {}^{172,174,176}\text{Hf}.$$

The small differences between $E_{\rm cal}$ and $E_{\rm exp}$ are caused mainly by the small residual interaction.

The situation is a little different for the low-lying $K^\pi = 8^-$ bands in ^{172,174,176}Hf. The overall agreement between the

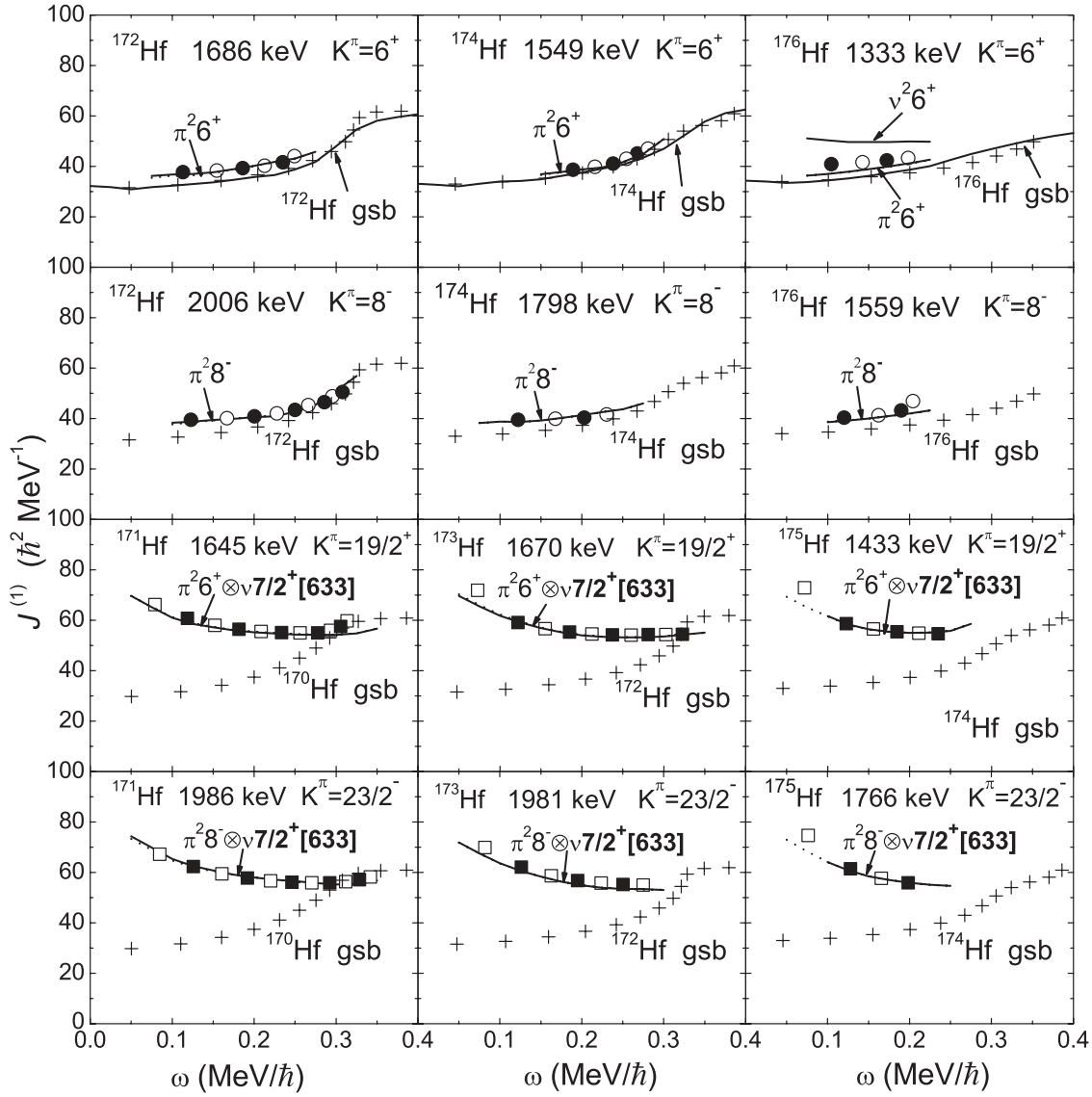

FIG. 7. MOIs of low-lying proton pair-broken bands $K^\pi = 6^+$, $\pi^2(7/2^+[404] \otimes 5/2^+[402])$, 8^-, $\pi^2(7/2^+[404] \otimes \mathbf{9/2^-[514]})$ in ^{172,174,176}Hf, and $K^\pi = 19/2^+$, $\pi^2 6^+ \otimes \nu\mathbf{7/2^+[633]}$ and $23/2^-$, $\pi^2 8^- \otimes \nu\mathbf{7/2^+[633]}$ in ^{171,173,175}Hf. The experimental MOIs of pair-broken bands in even-even nuclei are denoted by ● ($\alpha = 0$), ○ ($\alpha = 1$), and those of odd-A nuclei by ■ ($\alpha = 1/2$), □ ($\alpha = -1/2$), respectively. The experimental MOI of the reference band is denoted by +. The calculated MOIs by the PNC calculation are denoted by solid lines ($\alpha = 0$, or $1/2$) and dotted lines ($\alpha = 1$, or $-1/2$). No significant signature splitting is found for either the experimental or calculated MOIs of high-K pair-broken bands.

experimental MOIs of these bands and the PNC calculations using the $\pi^2 8^-(7/2^+[404] \otimes \mathbf{9/2^-[514]})$ configuration (Fig. 7) shows that the intrinsic configuration of low-lying $K^\pi = 8^-$ bands in ^{172,174,176}Hf may be of rather pure $\pi^2 8^-$. Dracoulis *et al.* [26] pointed out that the magnitude of neutron admixture is expected to be less for the $K^\pi = 8^-$ bands than for the $K^\pi = 6^+$ bands in the even-even Hf isotopes. In fact, because of the appearance of the small gap at $N = 104$ in the neutron Nilsson level scheme [Fig. 2(b)], the $\nu^2 8^-(7/2^-[514] \otimes \mathbf{9/2^+[624]})$ excitation is relatively high for $N \leqslant 104$ nuclei.

The experimental MOIs of $K^\pi = 6^+$ bands in ^{172,174}Hf are almost equal to that of the corresponding reference band ($K^\pi = 0^+, \alpha = 0$, gsb of adjacent even-even nuclei). The microscopic mechanism of the "identical 2-qp band" in the PNC formalism is very clear; i.e., the Coriolis responses of two unpaired protons in the deformation-aligned orbitals $\pi 7/2^+[404]$ ($g_{7/2}$) and $\pi 5/2^+[402]$ ($d_{5/2}$) are negligibly small, thus their blocking effects have little effect on the MOI. For comparison, both the experimental and calculated MOIs of the $K^\pi = 8^-$ bands in ^{172,174,176}Hf are a little larger than that of the reference band, because the blocking effect of the odd proton in the high-j (but high-Ω) orbital $\pi\mathbf{9/2^-[514]}$ ($h_{11/2}$) has a smaller influence on the MOI.

For the pair-broken (3-qp) bands $K^\pi = 19/2^+$ in ^{171,173,175}Hf, the PNC calculated MOIs using $\pi^2 6^+ \otimes \nu\mathbf{7/2^+[633]}$ agree very well with the experimental results, which in turn confirms the configuration assignment made

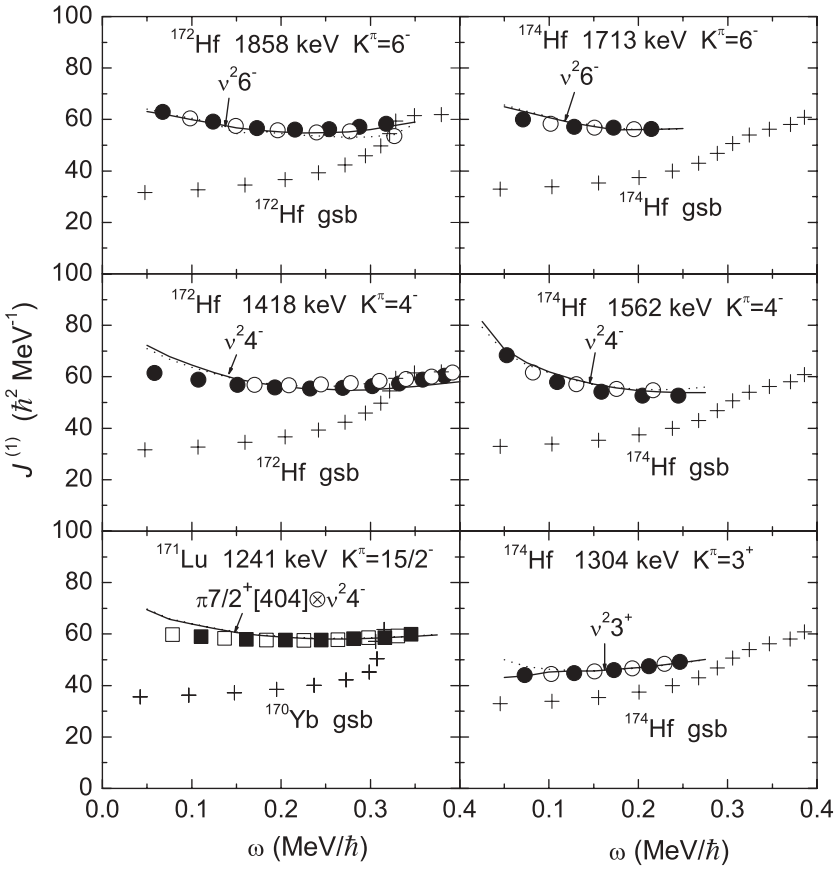

FIG. 8. Same as Fig. 7, but for the MOIs of low-lying neutron pair-broken bands. Notes: $\nu^2 6^-(\mathbf{7/2}^+[\mathbf{633}] \otimes 5/2^+[512])$, $\nu^2 4^-(\mathbf{7/2}^+[\mathbf{633}] \otimes 1/2^-[521])$, $\nu^2 3^+(5/2^+[512] \otimes 1/2^-[521])$.

in Refs. [18,23–26]. Similarly, the experimental MOIs of $K^\pi = 23/2^-$ bands in ^{171,173,175}Hf are nicely reproduced by the PNC calculations using the configuration $\pi^2 8^- \otimes \nu\mathbf{7/2}^+[\mathbf{633}]$. Unlike the analogous $K^\pi = 6^+$ and 8^- states in the adjacent even-even Hf nuclei without the spectator neutron $\nu\mathbf{7/2}^+[\mathbf{633}]$, both the experimental and calculated MOIs for the $K^\pi = 19/2^+$ and $23/2^-$ bands are much larger than that of the reference band at low ω, which is attributed to the blocking effect of the neutron high-j intruder orbital $\nu\mathbf{7/2}^+[\mathbf{633}]$ ($i_{13/2}$). The contribution of the neutron admixture $\nu^2 6^+$ to the MOI seems to be overshadowed by the strong blocking effect of $\nu\mathbf{7/2}^+[\mathbf{633}]$. However, the difference between the MOIs of $K^\pi = 19/2^+$ and $23/2^-$ bands and that of the reference band decreases gradually with increasing ω, and vanishes at $\hbar\omega > 0.3$ MeV because of the strong antipairing Coriolis interaction.

2. Low-lying high-K neutron pair-broken bands

As seen in Fig. 8, the experimental MOIs of the low-lying high-K neutron pair-broken bands are also well reproduced by the PNC calculations using appropriate configurations.

The MOIs of the $K^\pi = 6^-$ band at 1856 keV in ^{172}Hf and $K^\pi = 6^-$ band at 1713 keV in ^{174}Hf are much larger than that of the reference band at low ω, thus their intrinsic configuration may be reasonably considered as of rather pure $\nu^2 6^-(\mathbf{7/2}^-[\mathbf{633}] \otimes 5/2^-[512])$ as expected [see Fig. 2(b)]. Similarly, the $K^\pi = 4^-$ band at 1418 keV in ^{172}Hf and $K^\pi = 4^-$ band at 1562 keV in ^{174}Hf may be assigned to be $\nu^2 4^-(\mathbf{7/2}^-[\mathbf{633}] \otimes 1/2^-[521])$ as expected [see Fig. 2(b)].

The MOI of the $K^\pi = 3^+$ band at 1304 keV in ^{174}Hf is only a little larger than that of the reference band and may be assigned to be the expected lowest-lying neutron pair-broken configuration $\nu^2 3^-(1/2^-[521]5/2^-[512])$ [see Fig. 2(b)].

The MOI of the $K^\pi = 15/2^-$ band at 1241 keV in ^{171}Lu is much larger than that of the reference band (gsb of ^{170}Yb), and may be assigned to be $\pi 7/2^+[404] \otimes \nu^2 4^-$, where the blocking effect of the high-j intruder orbital $\nu\mathbf{7/2}^-[\mathbf{633}]$ plays an important role [29]. The $K^\pi = 13/2^+$ band at 1077 keV in ^{173}Hf may be considered as of the expected lowest three-quasineutron state, $\nu^3 13/2^+(\mathbf{7/2}^-[\mathbf{633}] \otimes 1/2^-[521] \otimes 5/2^-[512])$, which will be addressed in Sec. V (see Fig. 12).

C. Nonadditivity in MOIs

Assuming J_0 is the bandhead MOI of the quasiparticle-vacuum band, $J_0(\mu)$ is the bandhead MOI of the 1-qp band with intrinsic state $\alpha_\mu^+|0\rangle\rangle$, $\mu = 1, 2, \ldots$, $J_0(1,2)$ is that of the 2-qp band with intrinsic state $\alpha_1^+\alpha_2^+|0\rangle\rangle$, and $J_0(1,2,3)$ is that of the 3-qp band with intrinsic sate $\alpha_1^+\alpha_2^+\alpha_3^+|0\rangle\rangle$, etc., we define

$$R_0(1,2)_{\rm exp} = \frac{[J_0(1) - J_0]_{\rm exp} + [J_0(2) - J_0]_{\rm exp}}{[J_0(1,2) - J_0]_{\rm exp}},$$
$$R_0(1,2,3)_{\rm exp} = \frac{\sum_{i=1}^{3}[J_0(i) - J_0]_{\rm exp}}{[J_0(1,2,3) - J_0]_{\rm exp}}. \quad (3)$$

In the BCS independent quasiparticle formalism [6,38]

$$R(1,2)|_{\rm BCS} = R(1,2,3)|_{\rm BCS} = 1, \quad (4)$$

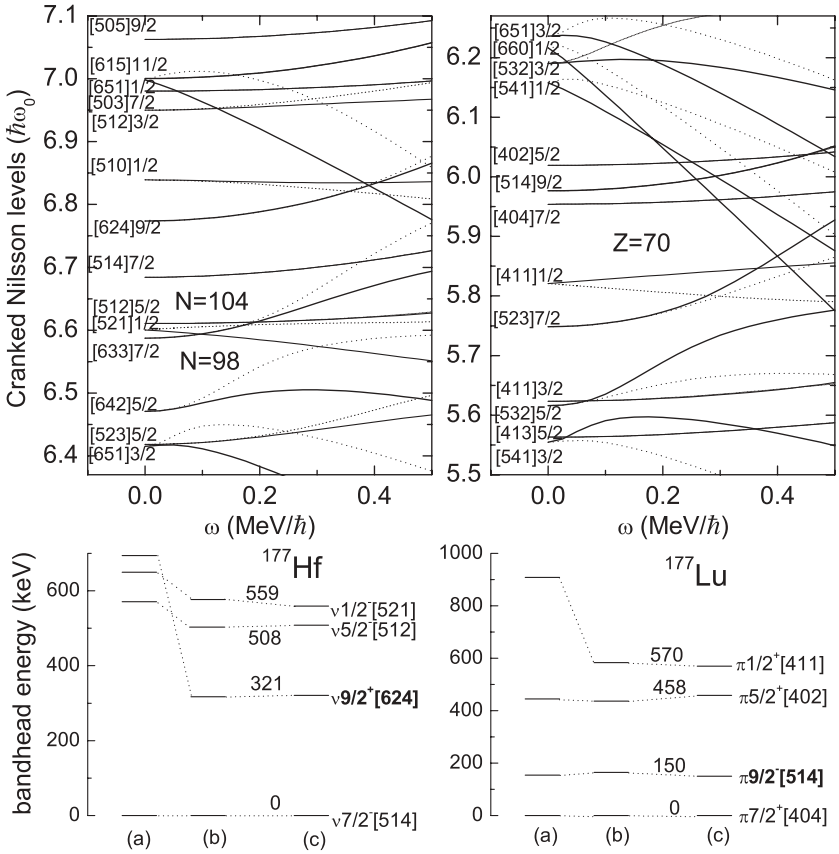

FIG. 9. Same as Figs. 3 and 4, but for the cranked Nilsson orbitals near the Fermi surface of ^{177}Hf and ^{177}Lu. The deformation parameters $(\varepsilon_2, \varepsilon_4)$ are taken from the Lund systematics [33]. $(\varepsilon_2, \varepsilon_4) = (0.254, 0.050)$ for ^{177}Hf, $(\varepsilon_2, \varepsilon_4) = (0.257, 0.057)$ for ^{177}Lu. The Nilsson parameters κ and μ (Lund systematics) are slightly adjusted to reproduce the bandhead energies of the low-lying 1-qp bands of ^{177}Hf and ^{177}Lu (see the lower part). For ^{177}Hf, $\kappa_5 = 0.0677$, $\kappa_6 = 0.0636$, $\mu_5 = 0.432$, $\mu_6 = 0.370$, and $1/2^-[510]$ is shifted downward by 0.090 $\hbar\omega_0$, $\mathbf{7/2^+[633]}$ upward by 0.01 $\hbar\omega_0$, $\mathbf{9/2^+[624]}$ upward by 0.024$\hbar\omega_0$. For ^{177}Lu, $\kappa_4 = 0.0610$, $\kappa_5 = 0.0600$, $\mu_4 = 0.609$, $\mu_5 = 0.609$, and $1/2^+[411]$ is further shifted upward by 0.023 $\hbar\omega_0$, $7/2^+[404]$ upward by 0.015 $\hbar\omega_0$. The effective pairing interaction strength is determined by the experimental odd-even difference in binding energies, $G_n = 0.32$ MeV for ^{177}Hf, $G_p = 0.32$ MeV for ^{177}Lu. (a), (b), (c) are the same as in Fig. 3.

i.e., there is additivity in MOIs, which is similar to the additivity in quasiparticle energies (note: the qp-vacuum energy is chosen as zero). However, all experimental results have

$$R(1,2)|_{\rm exp} > 1, \quad R(1,2,3)|_{\rm exp} > 1. \tag{5}$$

Some typical examples are given in Table I. In the BCS formalism, the nonadditivity in MOIs is attributed to the residual quasiparticle-quasiparticle interaction. However, the terms involving four creation and/or annihilation quasiparticle operators in the Hamiltonian, $H_{40} + H_{31} + H_{11}$, are very difficult to address and are usually neglected [39]. In fact, the experimental nonadditivity is mainly caused by the *destructive interference of blocking effects*, from which we have $[J_0(1,2) - J_0]_{\rm exp} < [(J_0(1) - J_0) + (J_0(2) - J_0)]_{\rm exp}$, $[J_0(1,2,3) - J_0]_{\rm exp} < [\sum_{i=1}^{3}(J_0(i) - J_0)]_{\rm exp}$, etc.; thus, $R(1,2)|_{\rm exp} > 1$, $R(1,2,3)|_{\rm exp} > 1$, etc. Considering that the experimental MOIs for various 1-qp and pair-broken bands can be well reproduced by the PNC calculations, the experimental nonadditivity in MOIs of multiquasiparticle (pair-broken) bands can also be well reproduced. In addition, we may define

$$R_0(1\ 2,\ 3)_{\rm exp} = \frac{[J_0(1,2) - J_0]_{\rm exp} + [J_0(3) - J_0]_{\rm exp}}{[J_0(1,2,3) - J_0]_{\rm exp}}, \tag{6}$$

TABLE I. Nonadditivity in MOIs of pair-excitation bands in Hf and Lu isotopes ($171 \leqslant A \leqslant 176$). The experimental low-lying $K^\pi = 8^-$ and $K^\pi = 6^+$ bands are assumed to be pure $\pi^2 6^+(7/2^+[404] \otimes 5/2^+[402])$ and $\pi^2 8^-(7/2^+[404] \otimes \mathbf{9/2^-[514]})$, respectively.

2-qp configuration	Two 1-qp configurations	$R(1,2)_{\rm exp}$	3-qp configuration	Three 1-qp configurations	$R(1,2,3)_{\rm exp}$	$R(1,2,3)_{\rm exp}$
^{172}Hf, $\pi^2 6^+$	^{171}Lu, $\pi 7/2^+$, $\pi 5/2^+$	1.37	^{171}Hf, $19/2^+$	^{171}Lu, $\pi 7/2^+$, $\pi 5/2^+$, ^{171}Hf, $\nu\mathbf{7/2^+}$	1.35	1.27
^{174}Hf, $\pi^2 6^+$	^{173}Lu, $\pi 7/2^+$, $\pi 5/2^+$	2.19	^{173}Hf, $19/2^+$	^{173}Lu, $\pi 7/2^+$, $\pi 5/2^+$, ^{173}Hf, $\nu\mathbf{7/2^+}$	1.27	1.13
^{176}Hf, $\pi^2 6^+$	^{175}Lu, $\pi 7/2^+$, $\pi 5/2^+$	1.62	^{175}Hf, $19/2^+$	^{175}Lu, $\pi 7/2^+$, $\pi 5/2^+$, ^{175}Hf, $\nu\mathbf{7/2^+}$	1.43	1.31
^{176}Hf, $\pi^2 6^+$	^{175}Lu, $\pi 7/2^+$, $\pi 5/2^+$	1.62	^{177}Hf, $19/2^-$	^{177}Lu, $\pi 7/2^+$, $\pi 5/2^+$, ^{177}Hf, $\nu 7/2^-$	1.56	1.15
^{172}Hf, $\pi^2 8^-$	^{171}Lu, $\pi 7/2^+$, $\pi\mathbf{9/2^-}$	2.19	^{171}Hf, $23/2^-$	^{171}Lu, $\pi 7/2^+$, $\pi\mathbf{9/2^-}$, ^{171}Hf, $\nu\mathbf{7/2^+}$	1.52	1.26
^{174}Hf, $\pi^2 8^-$	^{173}Lu, $\pi 7/2^+$, $\pi\mathbf{9/2^-}$	2.27	^{173}Hf, $23/2^-$	^{173}Lu,$\pi 7/2^+$, $\pi\mathbf{9/2^-}$, ^{173}Hf, $\nu\mathbf{7/2^+}$	1.47	1.24
^{176}Hf, $\pi^2 8^-$	^{175}Lu, $\pi 7/2^+$, $\pi\mathbf{9/2^-}$	2.12	^{175}Hf, $23/2^-$	^{175}Lu,$\pi 7/2^+$, $\pi\mathbf{9/2^-}$, ^{175}Hf, $\nu\mathbf{7/2^+}$	1.41	1.24
^{176}Hf, $\pi^2 8^-$	^{175}Lu, $\pi 7/2^+$, $\pi\mathbf{9/2^-}$	2.12	^{177}Hf, $23/2^+$	^{177}Lu,$\pi 7/2^+$, $\pi\mathbf{9/2^-}$, ^{177}Hf, $\nu 7/2^-$	1.54	1.28
^{176}Hf, $\pi^2 8^-$	^{175}Lu, $\pi 7/2^+$, $\pi\mathbf{9/2^-}$	2.12	^{177}Hf, $25/2^-$	^{177}Lu,$\pi 7/2^+$, $\pi\mathbf{9/2^-}$, ^{177}Hf, $\nu\mathbf{9/2^+}$	1.60	1.42

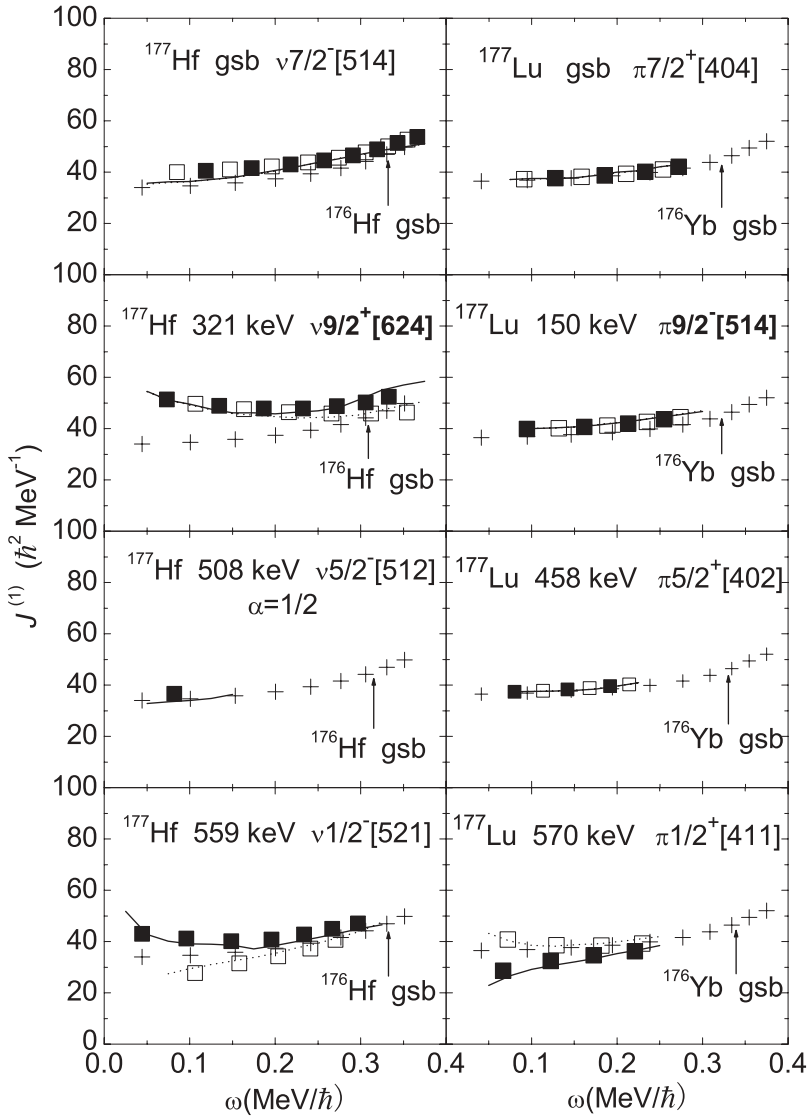

FIG. 10. MOIs of the low-lying 1-qp bands in ^{177}Hf and ^{177}Lu. The experimental MOIs are denoted by ■ ($\alpha = 1/2$) and □ ($\alpha = -1/2$), respectively. The calculated MOIs by PNC method are denoted by solid lines ($\alpha = 1/2$) and dotted lines ($\alpha = -1/2$), respectively. The experimental MOI of the reference band is denoted by +.

one can show $R(1\ 2,3)|_{\rm BCS} = 1$. Considering $R(1,2)|_{\rm exp} > 1$, $R(1,2,3)|_{\rm exp} > 1$, we have

$$R(1,2,3)|_{\rm exp} > R(1\ 2,3)|_{\rm exp} > 1, \qquad (7)$$

which is also verified by all experimental data (see Table I, last two columns).

IV. LOW-LYING BANDS IN ^{177}Hf, ^{177}Lu, AND ^{178}Hf

A. 1-qp bands in ^{177}Hf and ^{177}Lu

The cranked neutron levels of ^{177}Hf and proton levels of ^{177}Lu near the Fermi surface are shown in Fig. 9. The simple shell model calculations (pairing interaction neglected) for the bandhead energies of one-quasiproton bands in ^{177}Hf and one-quasiproton bands in ^{177}Lu are shown in the lower part of Fig. 9, column (a). The PNC calculations for the bandhead energies are shown in column (b). The neutron (proton) pairing interaction strength $G_n(G_p)$ is determined by the experimental odd-even difference in binding energies. The experimental bandhead energies of the 1-qp bands in ^{177}Hf and ^{177}Lu [column (c)] are well reproduced in PNC calculations.

The experimental and calculated MOIs of low-lying 1-qp bands in ^{177}Hf and ^{177}Lu are shown in Fig. 10.

The experimental MOIs of the one-quasiproton bands $\pi 7/2^+[404]$ and $\pi 5/2^+[402]$ in ^{177}Lu are almost "identical" to that of the reference band (Fig. 10), because both blocked orbitals $\pi 7/2^+[404]$ and $\pi 5/2^+[402]$ are deformation aligned orbitals with negligibly small Coriolis response. On the contrary, the MOI of the band $K^\pi = 9/2^+$ at 321 keV in ^{177}Hf is significantly larger than that of the reference band at low ω, because the blocked $\nu\mathbf{9/2^+[624]}$ ($i_{13/2}$) is a high-j intruder orbital. However, with increasing ω the odd-even difference in MOIs becomes smaller and smaller because of the large antipairing Coriolis interaction.

An obvious signature splitting is observed for the two $K = 1/2$ bands at 559 keV in ^{177}Hf and at 570 keV in ^{177}Lu, which is also well reproduced by PNC calculation. This is understandable from the behaviors of the $\Omega = 1/2$ cranked Nilsson neutron orbital $\nu 1/2^-[521]$ and proton orbital $\pi 1/2^+[411]$ (see Fig. 9). For the $K^\pi = 9/2^+$ band at 321 keV

in ^{177}Hf, obvious signature splitting appears only at $\omega > 0.20$ MeV, where the mixing between the high-j intruder $\nu\mathbf{7/2}^+[\mathbf{633}]$ and $\nu\mathbf{9/2}^+[\mathbf{624}]$ plays an important role.

B. Low-lying pair-broken bands in ^{177,178}Hf and ^{177}Lu

The PNC calculations for the MOIs of low-lying pair-broken (2-qp) bands in ^{178}Hf and the related pair-broken (3-qp) bands in ^{177}Hf and ^{177}Lu are given in Fig. 11.

For the lighter Hf isotopes ($N \leqslant 104$, ^{170,172,174,176}Hf), the neutron pair-broken excitation $\nu^2 8^-(7/2^-[514] \otimes \mathbf{9/2}^+[\mathbf{624}])$ is relatively high because of the subshell effect [Fig. 2(b)], thus the mixing between the $\nu^2 8^-$ and the low-lying proton pair-broken excitation $\pi^2 8^-(7/2^+[404] \otimes \mathbf{9/2}^-[\mathbf{514}])$ is expected to be weak for the low-lying $K^\pi = 8^-$ bands. For ^{177,178}Hf and ^{177}Lu ($N \geqslant 105$), $\nu^2 8^-$ is the lowest lying neutron pair-broken excitation [Fig. 2(b)], and it is expected that $\nu^2 8^-$ and $\pi^2 8^-$ should be strongly mixed. Indeed, two $K^\pi = 8^-$ bands (8_1^- at 1147 keV and 8_2^- at 1479 keV) were observed in ^{178}Hf [21,22], and both $K^\pi = 8^-$ bands were considered as admixtures of $\nu^2 8^-$ and $\pi^2 8^-$. The PNC calculations of MOIs for ^{178}Hf using pure $\nu^2 8^-$ and $\pi^2 8^-$ configurations are shown in Fig. 11. It is found that the experimental MOIs of 8_1^- and 8_2^- bands cannot be well reproduced by PNC calculations using pure $\nu^2 8^-$ or $\pi^2 8^-$ configuration, which supports the statement that both 8_1^- and 8_2^- bands in ^{178}Hf are the admixture of $\nu^2 8^-$ and $\pi^2 8^-$. Considering in ^{178}Hf the $\nu^2 8^-$ excitation is lower than $\pi^2 8^-$, the main component of the $K^\pi = 8_1^-$ band is expected to be $\nu^2 8^-$, particularly at low ω. This is not clear in the PNC calculations for the MOIs. Further investigation is necessary, with the neutron-proton residual interaction being considered.

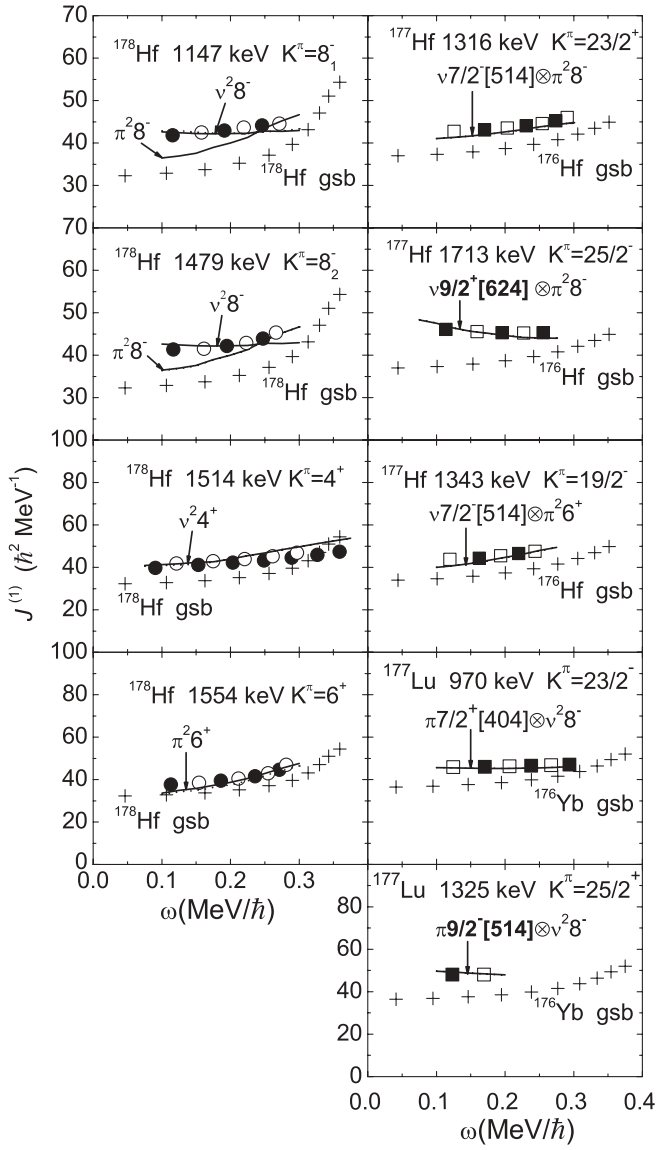

FIG. 11. MOIs of the low-lying pair-broken (2-qp) bands in ^{178}Hf, air-broken (3-qp) bands in ^{177}Hf and ^{177}Lu. The experimental MOIs are denoted by ● ($\alpha = 0$), ○ ($\alpha = 1$) for even-even nuclei, and by ■ ($\alpha = 1/2$) and □ ($\alpha = -1/2$) for odd-A nuclei. The calculated MOIs by the PNC calculation are denoted by solid lines ($\alpha = 0$ or $\alpha = 1/2$) and dotted lines ($\alpha = 1$ or $\alpha = -1/2$). No obvious signature splitting is found. Notes: $\pi^2 8^-(7/2^+[404] \otimes \mathbf{9/2}^-[\mathbf{514}])$, $\pi^2 6^+(7/2^+[404] \otimes 5/2^+[402])$, $\nu^2 8^-(7/2^-[514] \otimes \mathbf{9/2}^+[\mathbf{624}])$, $\nu^2 4^+(1/2^-[521] \otimes 7/2^-[514])$.

The low-lying 3-qp bands $K^\pi = 23/2^+$ at 1316 keV and $K^\pi = 25/2^-$ at 1713 keV in ^{177}Hf are analogous to the proton pair-broken $K^\pi = 8^-$ band at 1559 keV in ^{176}Hf (see Fig. 7) except for the spectator neutron $\nu 7/2^-[514]$ or $\nu\mathbf{9/2}^+[\mathbf{624}]$, respectively. Note that for the $K^\pi = 23/2^+$ and $25/2^-$ states in ^{177}Hf, the neutron pair-broken configuration $\nu^2 8^-$ is ruled out by the Pauli principle [27]. Thus we can understand why the experimental MOIs of both $K^\pi = 23/2^+$ and $K^\pi = 25/2^-$ bands are well reproduced by PNC calculations using the configurations $\nu 7/2^-[514] \otimes \pi^2 8^-$ and $\nu\mathbf{9/2}^+[\mathbf{624}] \otimes \pi^2 8^-$, respectively (Fig. 11).

The low-lying 3-qp bands $K^\pi = 23/2^-$ at 970 keV and $K^\pi = 25/2^+$ at 1325 keV in ^{177}Lu are similar to the neutron pair-broken band $\nu^2 8^-(7/2^-[514] \otimes \mathbf{9/2}^+[\mathbf{624}])$ in ^{178}Hf except for a spectator proton $\pi 7/2^+[404]$ and $\pi\mathbf{9/2}^-[\mathbf{514}]$, respectively. For the pair-broken (3-qp) bands $K^\pi = 23/2^-$ and $K^\pi = 25/2^+$ in ^{177}Lu, the proton pair-broken configuration $\pi^2 8^-(7/2^+[404] \otimes \pi\mathbf{9/2}^-[\mathbf{514}])$ is ruled out by the Pauli principle [32]. The PNC calculations for MOIs using the configurations $\pi 7/2^+[404] \otimes \nu^2 8^-$ and $\pi\mathbf{9/2}^-[\mathbf{514}] \otimes \nu^2 8^-$ agree well with the experimental results (Fig. 11), thus confirming the configuration assignments [32].

The experimental MOI of the $K^\pi = 6^+$ band at 1554 keV in ^{178}Hf is rather well reproduced using the lowest pair-broken configuration $\pi^2 6^+(7/2^+[404] \otimes 5/2^+[402])$ [Fig. 2(a)]. The possible mixing with $\nu^2 6^+(5/2^-[512] \otimes 7/2^-[514])$ seems to be small, because the configuration energy for $\nu^2 6^+$ is relatively high [see Fig. 2(b)]. The 3-qp band $K^\pi = 19/2^-$ at 1343 keV in ^{177}Hf is analogous to the $\pi^2 6^+$ state at 1554 keV in ^{176}Hf except for a spectator neutron $\nu 7/2^-[514]$. The calculation of MOIs for the $K^\pi = 19/2^-$ confirms the assigned configuration $\pi^2 6^+ \otimes \nu 7/2^-[514]$ [27].

For the $K^\pi = 4^+$ band at 1514 keV in ^{178}Hf, there are two possible low-lying pair-broken configurations [Fig. 2(b)], i.e., $\nu^2 4^+(1/2^-[521] \otimes 7/2^-[514])$ (triplet) and $\pi^2 4^+(\mathbf{9/2}^-[\mathbf{514}] \otimes \mathbf{1/2}^-[\mathbf{541}])$ (singlet). The calculated MOI for the configuration $\nu^2 4^+$ is closer to the experimental results (Fig. 11). Thus the main configuration of the $K^\pi = 4^+$ band may be $\nu^2 4^+$.

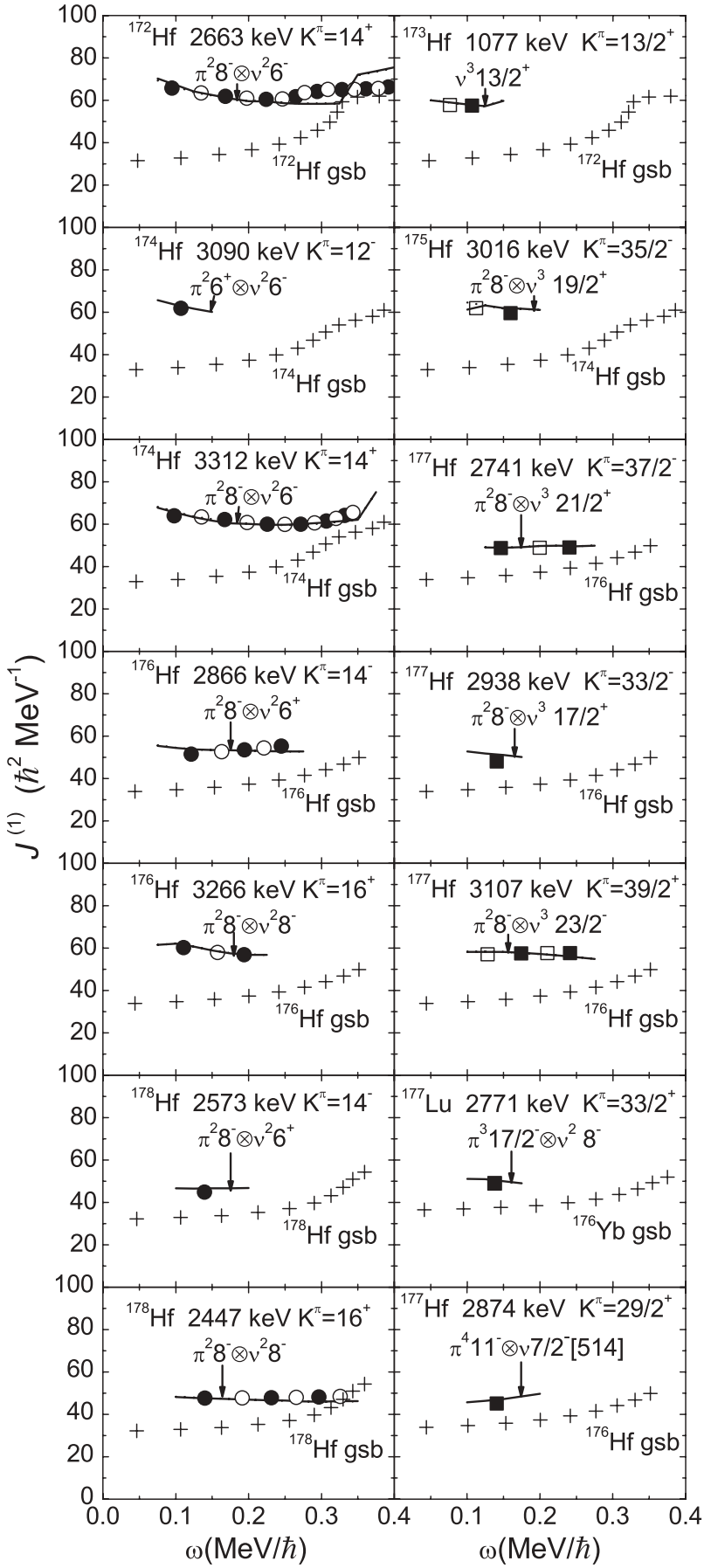

FIG. 12. MOIs of 2-pair-broken (4-qp) bands in even-even Hf isotopes, and multiquasiparticle bands in the odd-A Hf and Lu isotopes with more than two blocked neutron (proton) orbitals. The experimental MOIs are denoted by ● ($\alpha = 0$) and ○ ($\alpha = 1$) for even-even nuclei, and by ■ ($\alpha = 1/2$) and □ ($\alpha = -1/2$) for odd-A nuclei. The PNC-calculated MOIs are denoted by solid lines ($\alpha = 0$ or 1/2) and dotted lines ($\alpha = 1$ or $-1/2$). No obvious signature splitting is found. Notes: $\nu^3 13/2^+$(**7**/**2**$^+$[**633**] ⊗ 1/2$^-$[521] ⊗ 5/2$^-$[512]), $\nu^3 19/2^+$(**7**/**2**$^+$[**633**] ⊗ 5/2$^-$[512] ⊗ 7/2$^-$[514]), $\nu^3 17/2^+$(7/2$^-$[514] ⊗ **9**/**2**$^+$[**624**] ⊗ 1/2$^-$[510]), $\nu^3 21/2^-$(5/2$^-$[512] ⊗ 7/2$^-$[514] ⊗ **9**/**2**$^+$[**624**]), $\nu^3 23/2^-$(**7**/**2**$^+$[**633**] ⊗ 7/2$^-$[514] ⊗ **9**/**2**$^+$[**624**]), $\pi^3 17/2^-$(1/2$^+$[411] ⊗ 7/2$^+$[404] ⊗ **9**/**2**$^-$[**514**]), $\pi^4 11^-$(1/2$^+$[411] ⊗ 7/2$^+$[404] ⊗ 5/2$^+$[402] ⊗ **9**/**2**$^-$[**514**]).

V. OTHER MULTIQUASIPARTICLE BANDS IN Hf AND Lu ISOTOPES

Several 2-pair-broken (4-qp) high-K bands were observed in ^{172,174,176,178}Hf. The PNC calculations of the MOIs agree well with the experimental results (left column of Fig. 12), which provide reliable supports of the configuration assignments suggested in Refs. [17–19,21,22,28]. No obvious signature splitting is found for these high-K 2-pair-broken bands.

For the 2-pair-broken bands in ^{174}Hf, $K^\pi = 12^-$ band at 3090 keV and $K^\pi = 14^+$ at 3312 keV, the calculated MOIs using the configurations $\pi^2 6^+ \otimes \nu^2 6^-$ and $\pi^2 8^- \otimes \nu^2 6^-$ agree very well with the experiments. Considering for the three 1-pair-broken bands in ^{174}Hf (Fig. 7), $K^\pi = 6^+$ at 1549 keV, $K^\pi = 8^-$ at 1798 keV, and $K^\pi = 6^-$ at 1713 keV, the experimental MOIs are well reproduced by calculation using the configurations $\pi^2 6^+$, $\pi^2 8^-$, and $\nu^2 6^-$, respectively, we believe that the assigned configurations for these 2-pair-broken bands in ^{174}Hf [18,40] are reasonable. In addition, the bandhead energy $E_{\rm exp}(14^+ \text{in } ^{174}\text{Hf}) = 3312$ keV is a little smaller than $[E_{\rm exp}(\pi^2 8^-) + E_{\rm exp}(\nu^2 6^-)] = 3511$ keV. The small difference ($\sim$200 keV) may come from the attractive neutron-proton residual interaction. A similar 2-pair-broken band $K^\pi = 14^+$ with the configuration $\pi^2 8^- \otimes \nu^2 6^-$ was found in ^{172}Hf [17]. The bandhead energy $E_{\rm exp}(14^+ \text{in } ^{172}\text{Hf}) = 3663$ keV is also a little lower than $[E_{\rm exp}(\pi^2 8^-) + E_{\rm exp}(\nu^2 6^-)] = 3864$ keV.

In ^{176}Hf ($N = 104$), due to the neutron subshell effect [Fig. 2(b)], the configuration energy of $\nu^2 6^-$ is rather high, whereas the configuration energies of $\nu^2 6^+(5/2^-[512] \otimes 7/2^-[514])$ and $\nu^2 8^-(7/2^-[514] \otimes \mathbf{9/2^+[624]})$ are relatively low. Indeed, 2-pair-broken bands $K^\pi = 14^-$ at 2886 keV and $K^\pi = 16^+$ at 3266 keV in ^{176}Hf were observed [19]. The PNC calculated MOIs using the configurations $\pi^2 8^- \otimes \nu^2 6^+$ and $\pi^2 8^- \otimes \nu^2 8^-$ agree with the experiments. Note that in ^{176}Hf, the sum of two bandhead energies $[E_{\rm exp}(\pi^2 8^-) + E_{\rm exp}(\nu^2 6^+) = 2892]$ keV is close to $E_{\rm exp}(14^-) = 2866$ keV, implying the residual proton-neutron interaction is small.

The 2-pair-broken band $K^\pi = 16^+(\pi^2 8^- \otimes \nu^2 8^-)$ was observed in both ^{176}Hf and ^{178}Hf [19,21,22]. The PNC calculated MOIs of the two $K^\pi = 16^+$ bands in ^{176}Hf and ^{178}Hf using the configuration $\pi^2 8^- \otimes \nu^2 8^-$ agree well with the experimental results (Fig. 12), thus confirming the configuration assignment. In ^{178}Hf ($N = 106$), $\nu^2 8^-(7/2^-[514] \otimes \mathbf{9/2^+[624]})$ is the lowest neutron pair-broken configuration [see Fig. 2(b)], whereas in ^{176}Hf, the $\nu^2 8^-$ configuration is relatively high. This is why the bandhead energies $E_{\rm exp}(16^+, ^{178}\text{Hf}) = 2477$ keV $\ll E_{\rm exp}(16^+, ^{176}\text{Hf}) = 3266$ keV.

Finally, we address several multiquasiparticle bands, of which over two neutron (proton) Nilsson orbitals near the Fermi surface are blocked. For the seven multiquasiparticle bands (the right column of Fig. 12), the experimental MOIs are well reproduced by the PNC calculations, which in turn confirm the configuration assignments [18,25–27]. It is expected that for these multiquasiparticle states, the gap parameters Δ_ν (neutron) and/or Δ_π (proton) should be significantly reduced due to blocking effects, which will be addressed elsewhere. In general, the experimental MOIs of these bands are obviously larger than that of the reference (qp-vacuum) band at low ω, particularly when a high-j intruder orbital (e.g., $\nu\mathbf{7/2^+[633]}$, $i_{13/2}$) is blocked. However, the experimental MOIs are still significantly smaller than the rigid-body value ($J_{\rm rig.}/\hbar^2 \sim 80$ MeV^{-1} for the well-deformed rare-earth nuclei, see p. 74 of Ref. [4]).

VI. SUMMARY

The systematically observed low-lying high-$K(K \geqslant 3)$ pair-broken bands in Hf and Lu isotopes ($170 \leqslant A \leqslant 178$) are consistently analyzed using the PNC method, in which the blocking effects of unpaired nucleons are treated exactly. The effective pairing interaction strength is determined by the experimental odd-even difference in nuclear binding energies. Once an appropriate Nilsson level scheme is adopted to best fit the experimental bandhead energies of 1-qp bands in an odd-A nucleus, the large amount of experimental MOIs of 1-qp and low-lying high-$K(K \geqslant 3)$ pair-broken bands in Hf and Lu can be well reproduced by PNC calculations, with no free parameter. In most cases, calculation confirms the configuration assignments in earlier works. PNC calculations also show that the experimental systematics of high-K bands in Hf and Lu isotopes can be understood from the subshell effects of both neutron and proton near the Fermi surface.

The occupation probabilities n_μ and their variation with ω for the Nilsson orbital μ near the Fermi surface are also given in PNC calculations. They are essential to the discussion of the pairing reduction due to rotation and blocking, e.g., the ω and seniority dependence of the gap parameter Δ, which will be addressed elsewhere.

ACKNOWLEDGMENTS

This work is supported by National Natural Science Foundation of China (10675006, 10675007, 10778613), and the 973 program (2008CB717803, 2008CB317102).

APPENDIX: BRIEF REVIEW OF THE PNC METHOD FOR CSM

The CSM Hamiltonian of an axially symmetric nucleus in the rotating frame is [14,41]

$$\begin{aligned} H_{\rm CSM} &= H_0 + H_P, \\ H_0 &= H_{\rm Nil} - \omega J_x, \end{aligned} \tag{A1}$$

where $H_0 = H_{\rm Nil} - \omega J_x$ is the one-body part of $H_{\rm CSM}$, $H_{\rm Nil}$ is the Nilsson Hamiltonian, and $-\omega J_x$ is the Coriolis interaction with cranking frequency ω about the rotating x axis (perpendicular to the nuclear symmetry z axis). H_P is the pairing interaction

$$H_P = -G \sum_{\xi\eta} a^+_\xi a^+_{\bar\xi} a_{\bar\eta} a_\eta, \tag{A2}$$

where $\bar{\xi}(\bar{\eta})$ labels the time-reversal state of Nilsson state $\xi(\eta)$, and G is the effective strength of the pairing interaction, which is determined by the experimental odd-even difference in binding energies.

The eigenstate of $H_{\rm CSM}$ is

$$|\psi\rangle = \sum_i C_i |i\rangle \quad (C_i \text{ real}), \tag{A3}$$

where $|i\rangle$ is a cranked MPC (CMPC, an eigenstate of the one-body operator H_0). The CSM Hamiltonian $H_{\rm CSM}$ is diagonalized in a sufficiently large CMPC space to obtain the low-lying excited eigenstates.

The angular momentum alignment of $|\psi\rangle$ is

$$\langle\psi|J_x|\psi\rangle = \sum_i C_i^2 \langle i|J_x|i\rangle + 2\sum_{i<j} C_i C_j \langle i|J_x|j\rangle, \tag{A4}$$

and the kinematic moment of inertia for state $|\psi\rangle$ is

$$J^{(1)} = \frac{1}{\omega}\langle\psi|J_x|\psi\rangle. \tag{A5}$$

The occupation probability n_μ of the cranked orbital $|\mu\rangle$ is $n_\mu = \sum_i |C_i|^2 P_{i\mu}$, where $P_{i\mu} = 1$ if $|\mu\rangle$ is occupied in $|i\rangle$, and $P_{i\mu} = 0$ otherwise.

For $H_{\rm CSM}$ in Eq. (A1), besides the space-reflection symmetry, we have $[R_x(\pi), H_0] = [R_x(\pi), H_{\rm CSM}] = 0$, where $R_x(\pi) = e^{-i\pi J_x}$ is the rotation of π around the x axis. For an even-even nucleus, $R_x(\pi)^2 = 1$, the eigenvalue of $R_x(\pi)$, r (signature) $= e^{-i\pi\alpha} = \pm 1$, or the signature exponent $\alpha = 0, 1$. For an odd-A nucleus, $R_x(\pi)^2 = -1$, $r = \pm i$, and $\alpha = \mp 1/2$. As $[J_x, J_z] \neq 0$, the signature scheme invalidates quantum number K (eigenvalue of J_z). Note $[J_x, J_z^2] = 0$, each CMPC $|i\rangle$ may be chosen as a simultaneous eigenstate of $(H_0, R_x(\pi), J_z^2)$. However, K is still commonly used as a convenient quantum number to label rotational bands of deformed nuclei. For the gsb of an even-even nucleus, parity $\pi = +$, $\alpha = 0$, $K = 0$, $I = 0, 2, 4, \ldots$ (note, K mixing may occur with increasing I or rotational frequency ω). For an odd-A nucleus, if the Nilsson orbital 1 is blocked by an unpaired particle, we have two sequences of rotational levels with $\pi = \pi_1$, $K = \Omega_1$, $\alpha = \pm 1/2$, and $I \geqslant K$. For a pair-broken (2-qp) band in an even-even nucleus, when the Nilsson orbitals 1 and 2 are blocked by two unpaired particles, we have four sequences of rotational levels, $\pi = \pi_1\pi_2$, $K = |\Omega_1 \pm \Omega_2|$, $\alpha = 0$, 1, and $I \geqslant K$. For a pair-broken (3-qp) band in an odd-A nucleus, when the Nilsson orbitals 1, 2, and 3 are blocked by three unpaired particles, we have eight sequences of rotational levels, $\pi = \pi_1\pi_2\pi_3$, $K = |\Omega_1 \pm \Omega_2 \pm \Omega_3|$, $\alpha = \pm 1/2$, and $I \geqslant K$. The situation is similar for 2-pair-broken bands, etc.

As we are only interested in the low-lying excited bands, the number of important CMPC (weight $> 1\%$, say) is very limited (usually <20) for the well-deformed rare-earth nuclei. In the present PNC calculation, the dimension of CMPC space is about 700 for proton and 800 for neutron. In fact, almost all the CMPCs with weight $>0.1\%$ are involved in the calculations, so the solutions to the low-lying excited states are accurate enough. With increasing dimension of the CMPC space, the effective pairing interaction strength decreases correspondingly, and the final calculated results almost remain the same. The stability of the calculation with respect to the basis cutoff has been illustrated in detail (see Refs. [7,41]).

[1] S. Singh, S. S. Malik, and A. K. Jain, At. Data Nucl. Data Tables **92**, 1 (2006).
[2] P. M. Walker, Phys. Scr. **T5**, 29 (1983).
[3] A. Bohr, B. R. Mottelson, and D. Pines, Phys. Rev. **110**, 936 (1958).
[4] A. Bohr and B. R. Mottelson, *Nuclear Structure, Nuclear Deformations*, Vol. II (Benjamin, New York, 1975).
[5] J. Y. Zeng, S. X. Liu, L. X. Gong, and H. B. Zhu, Phys. Rev. C **65**, 044307 (2002).
[6] J. Y. Zeng and T. S. Cheng, Nucl. Phys. **A405**, 1 (1983).
[7] H. Molique and J. Dudek, Phys. Rev. C **56**, 1795 (1997).
[8] R. W. Richardson, Phys. Rev. **141**, 949 (1966).
[9] B. R. Mottelson and J. G. Valatin, Phys. Rev. Lett. **5**, 511 (1960).
[10] L. F. Canto, P. Ring, and J. O. Rasmussen, Phys. Lett. **B161**, 21 (1985).
[11] D. J. Rowe, *Nuclear Collective Motion* (Methuen, London, 1970).
[12] G. Dracoulis, F. G. Kondev, and P. M. Walker, Phys. Lett. **B419**, 7 (1998).
[13] J. Y. Zeng, T. S. Cheng, L. Cheng, and C. S. Wu, Nucl. Phys. **A421**, 125 (1984).
[14] J. Y. Zeng, T. H. Jin, and Z. J. Zhao, Phys. Rev. C **50**, 1388 (1994).
[15] P. M. Walker *et al.*, Phys. Rev. Lett. **65**, 416 (1990).
[16] P. M. Walker and G. D. Dracoulis, Nature **399**, 35 (1999).
[17] D. M. Cullen *et al.*, Phys. Rev. C **52**, 2415 (1995).
[18] N. L. Gjørup *et al.*, Nucl. Phys. **A582**, 369 (1995).
[19] T. L. Khoo, F. M. Bernthal, R. G. H. Robertson, and R. A. Warner, Phys. Rev. Lett. **37**, 823 (1976).
[20] P. M. Walker, G. D. Dracoulis, A. Johnson, and J. R. Leigh, Nucl. Phys. **A293**, 481 (1983).
[21] S. M. Mullins *et al.*, Phys. Lett. **B393**, 279 (1997).
[22] A. B. Hayes *et al.*, Phys. Rev. Lett. **89**, 242501 (2002).
[23] G. Dracoulis and P. M. Walker, Nucl. Phys. **A330**, 186 (1979).
[24] D. M. Cullen, D. E. Appelbe, A. T. Reed, C. Baktash, and C. H. Yu, Phys. Rev. C **55**, 508 (1997).
[25] B. Fabricius *et al.*, Nucl. Phys. **A523**, 426 (1991).
[26] G. Dracoulis and P. M. Walker, Nucl. Phys. **A342**, 335 (1980).
[27] S. M. Mullins, A. P. Byrne, G. D. Dracoulis, T. R. McGoram, and W. A. Seale, Phys. Rev. C **58**, 831 (1998).
[28] S. M. Mullins *et al.*, Phys. Lett. **B400**, 401 (1997).
[29] R. A. Bark *et al.*, Nucl. Phys. **A644**, 29 (1998).
[30] P. Petkov *et al.*, Nucl. Phys. **A599**, 505 (1996).
[31] P. E. Garrett *et al.*, Phys. Rev. C **69**, 017302 (2004).
[32] G. Dracoulis *et al.*, Phys. Lett. **B584**, 22 (2004).
[33] R. Bengtsson, S. Fraundorf, and F. R. May, At. Data Nucl. Data Tables **35**, 15 (1986).
[34] S. G. Nilsson *et al.*, Nucl. Phys. **A131**, 1 (1969).
[35] F. G. Kondev *et al.*, Nucl. Phys. **A617**, 91 (1997).
[36] C. J. Gallagher, Phys. Rev. **126**, 1525 (1962).

[37] C. Baktash, J. D. Garrett, D. F. Winchell, and A. Smith, Phys. Rev. Lett. **69**, 1500 (1992).
[38] S. X. Liu and J. Y. Zeng, Phys. Rev. C **66**, 067301 (2002).
[39] S. G. Nilsson and O. Prior, Mat. Fys. Medd. K. Dan. Vidensk. Selsk. **32**, 16 (1961).
[40] *Table of Isotopes: 1999 Update with CD-ROM*, 8th ed., edited by R. Firestone, C. M. Baglin, and S. Y. Frank Chu (Wiley, New York, 1999).
[41] S. X. Liu, J. Y. Zeng, and E. G. Zhao, Phys. Rev. C **66**, 024320 (2002).